Flexible usage and interconnectivity of diverse cell death pathways protects against intracellular infection

Marcel Doerflinger[1,2,12], Yexuan Deng[1,3,12], Paul Whitney[2,4,12], Ranja Salvamoser[1,2,12], Sven Engel[2,4], Andrew J Kueh[1,2], Lin Tai[1], Annabell Bachem[2,4], Elise Gressier[2,4], Niall Geoghegan[1,2], Stephen Wilcox[1,2], Kelly Rogers[1,2], Alexandra L. Garnham[1,2], Michael A. Dengler[1,2], Stefanie M. Bader[1], Gregor Ebert[1,2], Jaclyn S. Pearson[5,6,7], Dominic De Nardo[1,2,8], Nancy Wang[2,4], Chenying Yang[2,4,9], Milton Pereira[10,11], Clare Bryant[11], Richard A. Strugnell[2,4], James E. Vince[1,2], Marc Pellegrini[1,2], Andreas Strasser[1,2,13,14*], Sammy Bedoui[2,4,13*] and Marco J Herold[1,2,13*]

[1]The Walter and Eliza Hall Institute of Medical Research, Parkville, VIC, Australia

[2]Department of Medical Biology, University of Melbourne, Parkville, VIC, Australia

[3]The State Key Laboratory of Pharmaceutical Biotechnology, School of Life Sciences, Nanjing University, Nanjing, China.

[4]Department of Microbiology and Immunology at the Doherty Institute for Infection and Immunity, The University of Melbourne, Parkville, VIC, Australia

[5]Centre for Innate Immunity and Infectious Diseases, Hudson Institute of Medical Research, Clayton, Victoria, Australia.

[6]Department of Molecular and Translational Research, Monash University, Clayton, VIC, Australia.

[7]Department of Microbiology, Monash University, Clayton, VIC, Australia

[8]Department of Anatomy and Developmental Biology, Monash Biomedicine Discovery Institute, Monash University, Clayton, VIC, Australia.

[9]Current address: Menzies Health Institute Queensland, Griffith University

[10]Division of Infectious Diseases and Immunology, University of Massachusetts Medical School, Worcester, MA, USA

[11]University of Cambridge, UK

[12]These authors contributed equally

[13]These authors contributed equally

[14]Lead Contact

*Correspondence: strasser@wehi.edu.au (A.S.), sbedoui@unimelb.edu.au (S.B.), herold@wehi.edu.au (M.J.H.).

Graphical Abstract

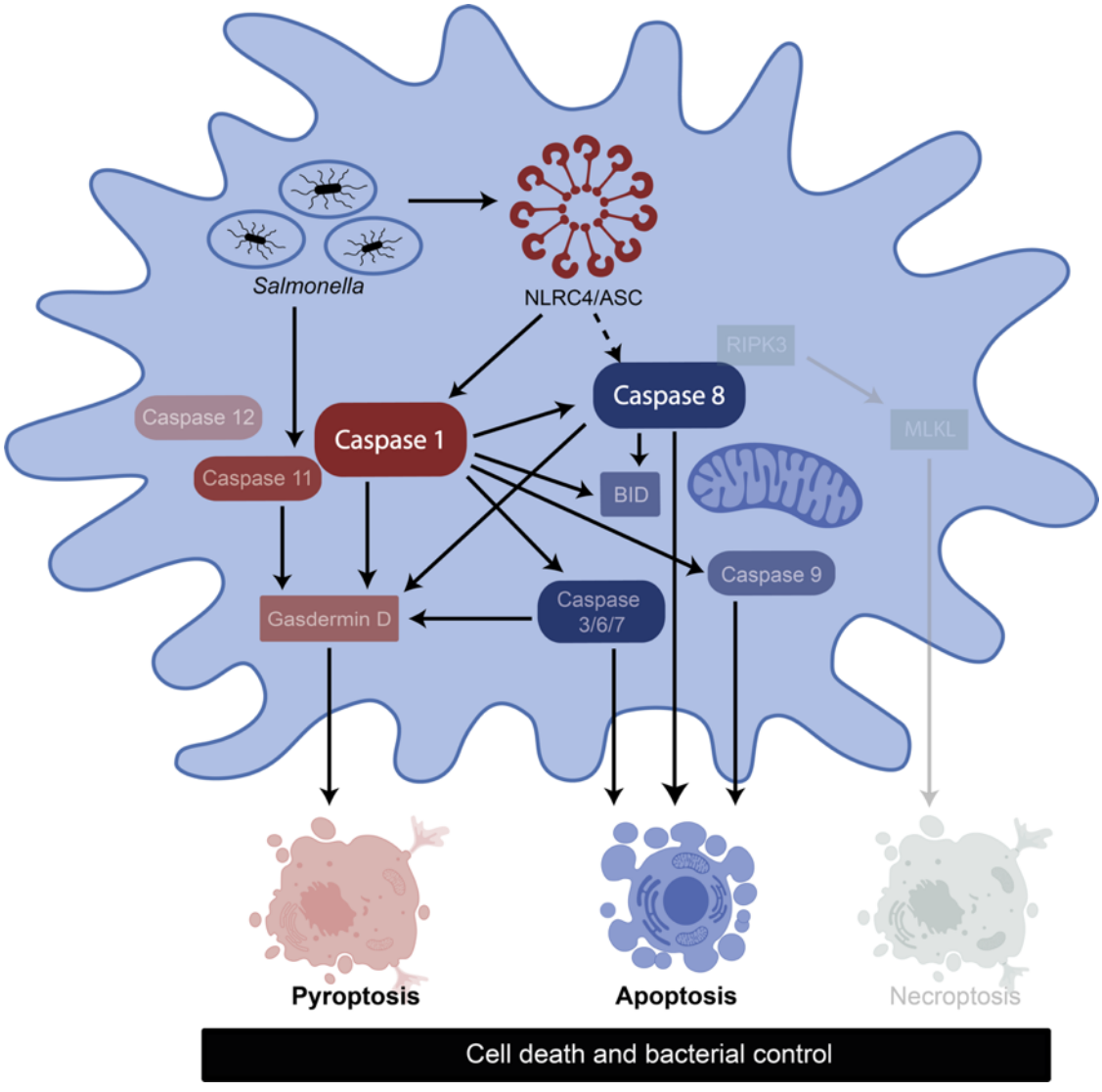

In Brief

Salmonella infection can no longer be controlled in mice lacking pyroptosis, apoptosis and necroptosis. Doerflinger et al. demonstrates that these cell death pathways are highly interconnected and used very flexibly. Furthermore, it is demonstrated that the initiators of pyroptosis and extrinsic apoptosis Caspase-1 and -8, respectively, can exert executioner functions in cell death themselves when all executioner proteins are lacking.

Highlights

- **Combined deletion of pyroptosis, apoptosis and necroptosis in mice leads to a failure to control Salmonella infection.**
- **BMDMs lacking caspase-1/11/12/8 and RipK3 are resistant to Salmonella induced killing.**
- **Caspase-1 is capable of killing cells through GSDMD, BID mediated intrinsic apoptosis and direct activation of caspase-3, -7 and -9.**
- **Caspase-1 and caspase-8 can act as executioners of cell death if all downstream effectors of cell death are deleted.**

SUMMARY

Apoptosis, pyroptosis and necroptosis contribute to host protection against diverse pathogens, but their interplay and the underlying molecular mechanisms coordinating their interactions have not yet been resolved (Green, 2019). To define the relative importance of these cell death pathways and their inter-connectivity in host defence, we deleted caspases-1/-11/-12/-8 and RIPK3 in varying combinations to generate mice lacking pyroptosis, death receptor-induced apoptosis and/or necroptosis, and subjected them to *Salmonella enterica* serovar Typhimurium (*S.* Typhimurium) infection. The loss of each cell death pathway alone had only minor impact on pathogen control but the combined absence of pyroptosis, caspase-8 mediated apoptosis and necroptosis led to a failure to clear the pathogen and consequently severe sickness of *Salmonella* infected *Casp1/11/12/8/Ripk3*$^{-/-}$mice. Bone marrow derived macrophages (BMDMs) lacking individual cell death pathways were potently killed upon *Salmonella* infection, while *Casp1/11/12/8/Ripk3*$^{-/-}$ BMDMs were fully resistant and failed to control intracellular bacterial growth, demonstrating that cells can employ varying cell death processes to limit intracellular infections. We show that this functional overlap between cell death pathways was afforded by extensive signaling cross-talk between the initiators and effectors of pyroptosis (caspase-1/11, GSDMD) and apoptosis (BID, BAX, BAK & caspases-3/6/7/8/9). Strikingly, *Salmonella* infection could kill BMDMs even in the absence of all known executioners of cell death as long as caspase-1 and caspase-8 were present, indicating that these caspases can act not only as initiators but also as executioners of cell death. These findings indicate that apoptosis, pyroptosis and to a lesser extent necroptosis constitute components of a highly intertwined and coordinated cell death system that provides the host with remarkable flexibility and fail-safe processes for the control of intracellular infections.

INTRODUCTION

Metazoans not only depend on the regulated division and multiplication of cells, but also require their coordinated removal through different types of programmed cell death (PCD), such as apoptosis, necroptosis and pyroptosis (Green, 2019). Cell demolition during apoptosis is executed by so-called effector caspases (caspase-3, -6 and -7) that promote cellular fragmentation into apoptotic bodies and engulfment of dying cells by neighbouring cells (Salvesen and Dixit, 1997). This facilitates the immunologically 'silent' removal of the remains of dead cells, thereby preventing lytic rupture that mediates release of intracellular content causing inflammation (Nagata, 2018). Apoptosis can be induced either by death receptors, such as FAS or TNFR1, that activate caspase-8, or through cellular stress via the intrinsic (also called BCL-2 regulated or mitochondrial) pathway involving BH3-only protein-initiated and BAX/BAK-mediated mitochondrial outer membrane permeabilization (MOMP) (Czabotar et al., 2014). This causes activation of the initiator caspase, caspase-9, and consequent activation of the effector caspases. Pyroptosis is induced through NLR-dependent activation of caspase-1 or LPS-induced activation of caspase-11 (Lamkanfi and Dixit, 2014; Zhao and Shao, 2016), while ligation of TNFR1 or Toll-like receptors (TLRs) causes phosphorylation of RIPK1 and RIPK3 to initiate necroptosis in the absence of caspase-8 activity (Ofengeim and Yuan, 2013; Vandenabeele et al., 2010). Interestingly, pyroptosis and necroptosis are both executed through large pores in the cell membrane that cause water influx, cellular swelling and loss of membrane potential. The cell bursts and exposes its content to the extracellular space, which can elicit a variety of pro-inflammatory responses priming both the innate as well as the adaptive immune systems. Although we know many details about the molecular circuits responsible for triggering these individual pathways of cellular suicide, it is not clear why so many seemingly parallel pathways have been conserved throughout evolution.

One important biological function of cellular suicide pertains to the role of programmed cell death (PCD) in controling intracellular pathogens (Jorgensen et al., 2017; Kayagaki et al., 2015; Shi et al., 2015). The killing of infected cells is thought to remove a replicative niche, re-expose the pathogen to extracellular immune effector mechanisms and make antigens available for triggering pathogen-specific adaptive immune responses. *Salmonella* has been widely used as a model for studying the role of programmed cell death in host defence (Broz et al., 2012; Franchi et al., 2009). This intracellular pathogen can cause typhoid fever, a systemic infection that affects 10-20 million people worldwide and kills >135,000 individuals per annum (Browne et al., 2020). The disease can be modeled by infecting mice with *S.* Typhimurium (Kupz et al., 2014) and spleen and liver are major sites of replication in systemic *Salmonella* infections. The primary target of *Salmonella* spp. are phagocytes, in which the bacteria survive by repurposing a host cell-derived membrane compartment into a specialized niche. Phagocytes, such as macrophages, respond to *Salmonella* infection through inflammasome formation involving NAIP2/5 and nucleotide-binding oligomerization domain-like receptors (NLR), such as NLRC4 and NLRP3 (Franchi et al., 2009; Miao et al., 2010), that activate caspase-1 (Zhang et al., 2015). The resulting proximity-induced activation of Caspase-1 causes the proteolytic maturation of the inflammatory cytokines IL-1β and IL-18 and releases N-terminal fragments of gasdermin D (GSDMD) that form pores in the cell membrane to elicit pyroptosis. Although these processes appear highly relevant *in vitro,* with caspase-1 or GSDMD-deficient phagocytes resisting *Salmonella*-induced cell death (Franchi et al., 2006; Mariathasan et al., 2004), *in vivo* studies suggest that *Salmonella* can be controlled in the absence of inflammasome-driven pyroptosis (Broz et al., 2010). This may reflect the capacity of the host to compensate for the lack of one type of cell death by using another. Such "fail-safe" systems have been hypothesized before and may represent the host's response to offset a variety of evasion strategies employed by pathogens to prevent immune recognition (Bedoui

et al., 2010). Very little is known about the organization, regulation and kinetics of such functional backup in the use of different programmed cell death pathways during host defence against pathogens *in vivo*. Here, we investigated the relative contributions of all initiator and executioner caspases and the cell death effectors they activate to provide host defence against systemic *Salmonella* infections.

RESULTS

Combined Loss of Caspase-1/11/12 and Caspase-8 Prevents *Salmonella*-Induced Cell Death and Impairs Bacterial Clearance *in vivo*

We infected C57BL/6 (wild-type: WT) mice with a growth-attenuated strain of *S.* Typhimurium that mirrors the systemic phase of typhoid fever (Kupz et al., 2014; Kupz et al., 2013). This infection follows a classical pattern where bacterial growth initially outpaces host defense. By about week 3, bacterial titers reach a peak that is followed by dropping titres and eventual clearance of the bacteria from the host. This type of infection thus allows detailed *in vivo* investigations into the mechanisms that enable control of this globally relevant intracellular pathogen by innate immune mechanisms over the first 3 weeks of the infection (Kupz et al., 2012; Kupz et al., 2013) and T cell-mediated immune clearance thereafter (Benoun et al., 2018). Consistent with earlier reports using WT strains of *S.* Typhimurium (Broz et al., 2012), we observed slightly elevated bacterial titres in *Casp1/11*$^{-/-}$ mice 3 weeks post-infection compared to WT controls (Figure 1A), but the lack of pyroptosis in these mice did not affect their capacity to clear the bacteria at 12-weeks post-infection, indicating a selective defect in bacterial control albeit minor in magnitude. Exploiting this *in vivo* model of caspase-1/11-independent bacterial control, we explored the role of other cell death pathways and their key constituents. We first investigated whether the lack of caspases-1 and -11 was compensated for by caspase-12, given their substantial amino acid similarity and chromosomal co-localization. However, at week 3 post-infection *Casp1/11/12*$^{-/-}$ and *Casp1/11*$^{-/-}$ mice presented with comparable minor increases in bacterial titres that were similar to those observed in WT controls (Figure 1B). This reveals that caspase-12 does not play a critical role in bacterial clearance *in vivo* by compensating for the combined absence of caspases-1 and -11.

Caspase-8 has been suggested to coordinate an alternative pathway towards pyroptotic cell death that operates independently of caspases-1/11 (Mascarenhas et al., 2017; Orning et al., 2018), which prompted us to investigate the contribution of caspase-8 driven cell death to *Salmonella* control in mice. To prevent the necroptosis-dependent embryonic lethality caused by loss of caspase-8, we used *Casp8/Ripk3*$^{-/-}$ mice (Alvarez-Diaz et al., 2016; Kaiser et al., 2011; Oberst et al., 2011). The lack of caspase-8-mediated apoptosis and RIPK3-driven necroptosis alone did not have any significant impact on *Salmonella* titres 3 weeks post-infection (Figure 1B), indicating that additional cell death processes were required for bacterial control. Interestingly, mice lacking necroptosis alone (*Mlkl*$^{-/-}$ mice) or even mice with combined deficiency in pyroptosis and necroptosis (*Casp1/11/12/Ripk3*$^{-/-}$ mice) had no defects in bacterial control until at least three weeks post-infection (Figure 1B and S1A). These findings demonstrate that mice with defects in select types of programmed cell death only have minor impairments in their ability to control bacterial replication.

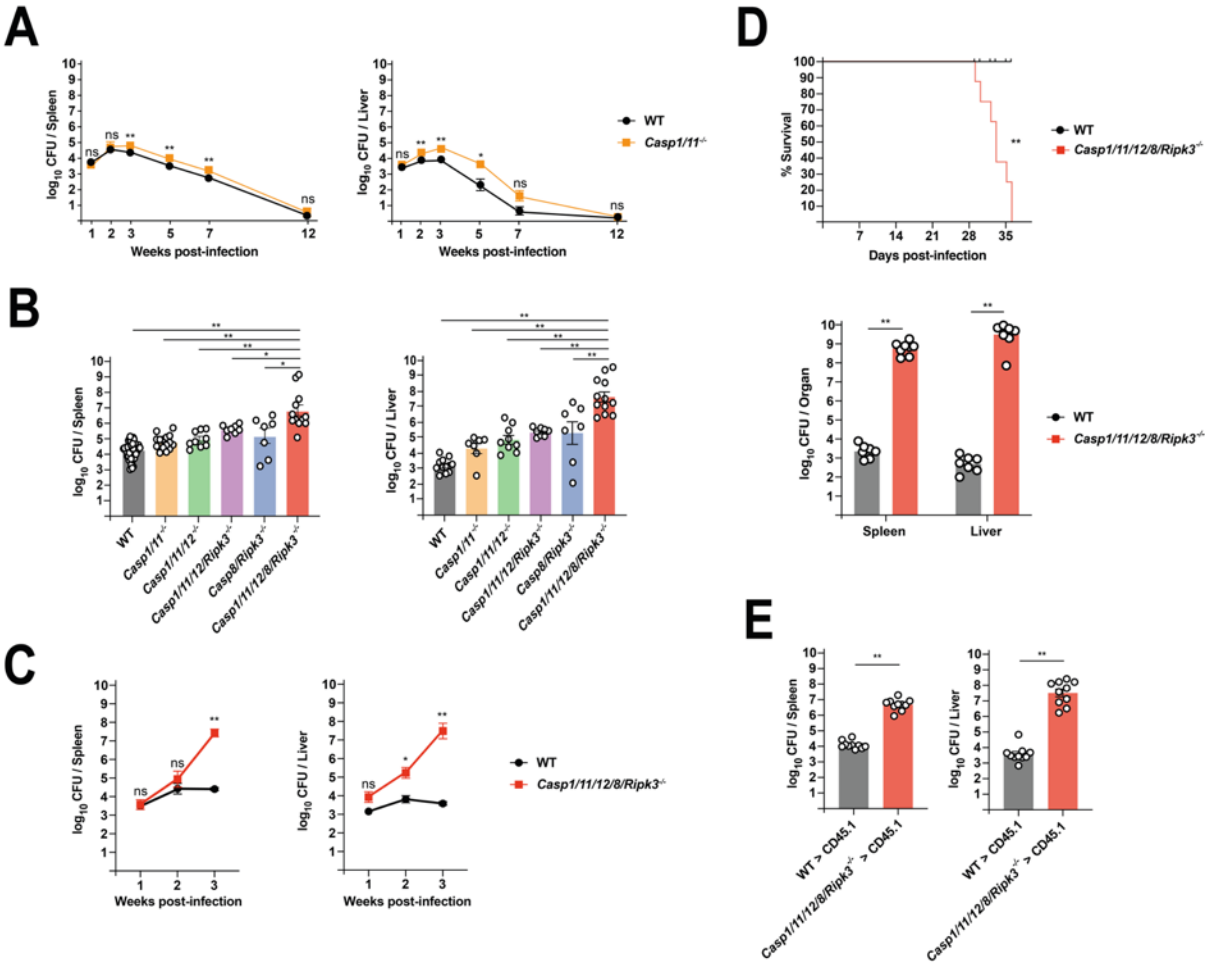

Figure 1. Combined Loss of Caspase-1/11/12 and Caspase-8 Leads to Lack of Bacterial Clearance upon *Salmonella* Infection.

(A) Clearance kinetics of WT and *Casp1/11*$^{-/-}$ mice infected with *Salmonella ΔAroA* (200 CFU). *N*=10-22 mice per group per time point. Mean and SEM are shown. **P<0.005, *P<0.05, ^{ns}P>0.05=not significant.

(B) Bacterial loads in spleen and liver 3 week post infection of WT, *Casp1/11*$^{-/-}$, *Casp1/11/12*$^{-/-}$, *Casp1/11/12/Ripk3*$^{-/-}$, *Casp8/Ripk3*$^{-/-}$ and *Casp1/11/12/8/Ripk3*$^{-/-}$ mice infected with *Salmonella ΔAroA* (200 CFU). *N*=7-48 mice per group. Mean and SEM are shown. **P<0.005, *P<0.05, ^{ns}P>0.05=not significant.

(C) Bacterial loads in spleen and liver from 1-week to 3-week post-infection of WT and *Casp1/11/12/8/Ripk3*$^{-/-}$ mice with *Salmonella ΔAroA* (200 CFU). *N*=3-4 mice per genotype and time point. Mean and SEM are shown. **P<0.005, *P<0.05, ^{ns}P>0.05=not significant.

(D) Mouse survival curves and corresponding bacterial loads in the spleen and the liver at time of sacrifice in WT and *Casp1/11/12/8/Ripk3*$^{-/-}$ mice infected with *Salmonella ΔAroA* (200 CFU). *N*=7-8 mice per group. Mean and SEM are shown. **P<0.005.

(E) Bone marrow chimeras of the indicated genotypes were infected with *Salmonella ΔAroA* (200 CFU) and culled for analysis of bacterial loads in spleen and liver 3 weeks post infection. *N*=10 mice per group. Mean and SEM are shown. **P<0.005.

These findings raised the possibility that *in vivo* control of *Salmonella* infection is safeguarded by extensive functional back-up between several programmed cell death processes. To investigate this directly, we generated *Casp1/11/12/8/Ripk3*$^{-/-}$ mice that are deficient for pyroptosis, extrinsic apoptosis and necroptosis. Strikingly, these mice had drastically elevated bacterial titres in their liver and spleen at week 2 and 3 post-infection, respectively, compared to WT animals (Figure 1B,C), and eventually succumbed to the infection between 4 and 5 weeks post-infection (Figure 1D). This shows that host defence against *Salmonella* necessitates the activity of at least one of these types of programmed cell death pathways and that none of the other known cell death pathways (e.g. intrinsic apoptosis or ferroptosis) were sufficient to ensure control of the infection in their absence. Of note, we observed similar defects in host defence in bone marrow chimeras in which pyroptosis, caspase-8-mediated apoptosis and necroptosis were only missing from the immune cell compartment (Figure 1E). Therefore, we conclude that *Salmonella* control broke down in *Casp1/11/12/8/Ripk3*$^{-/-}$ mice because phagocytes could no longer purge the bacteria from their vacuolar compartments by undergoing programmed cell death.

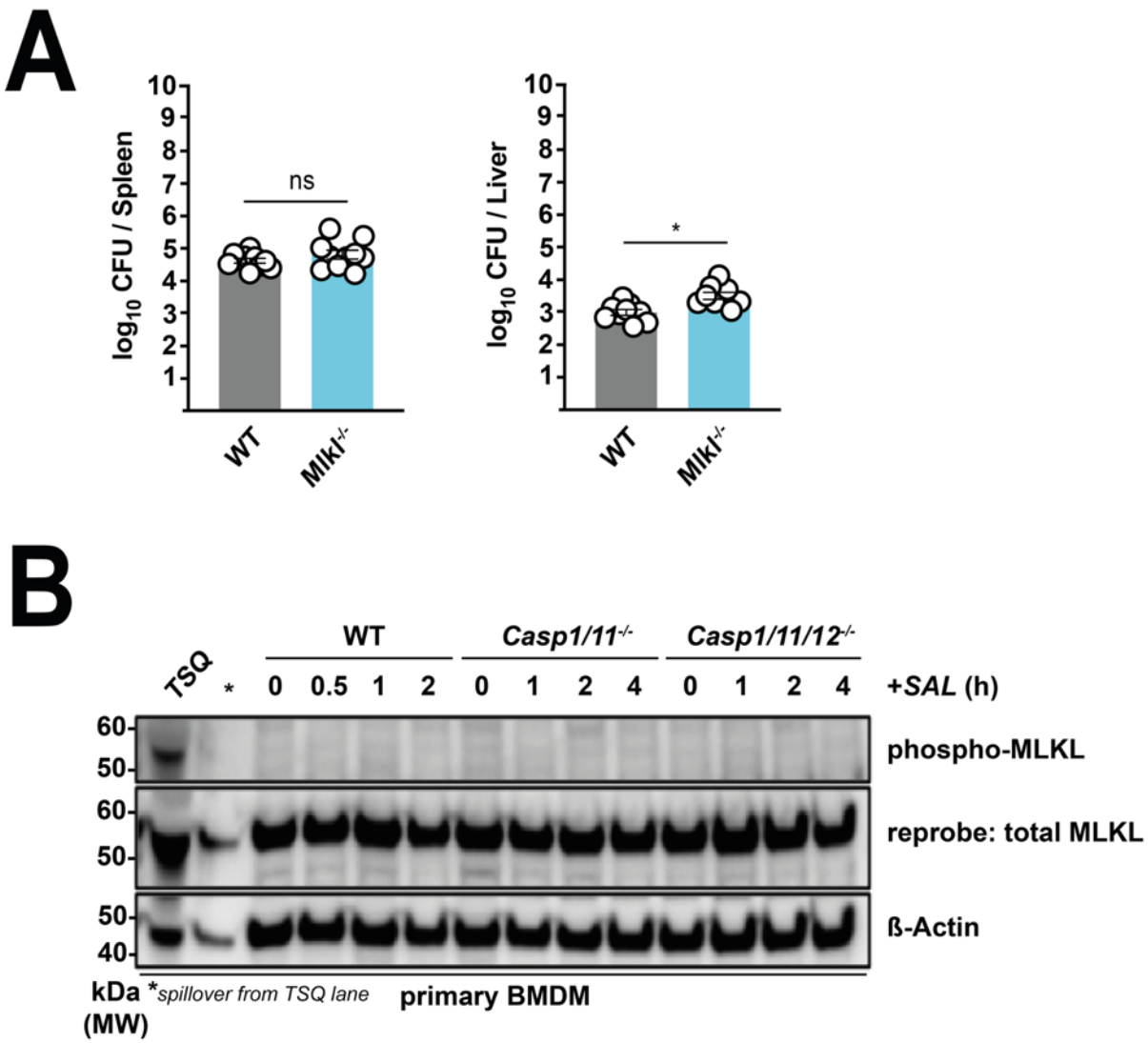

Figure S1: Necroptosis Does Not Affect Bacterial Clearance or Provide Back-up for Loss of Pyroptosis

(A) Bacterial loads in spleen and liver 3-week post infection in WT, and *Mlkl*$^{-/-}$ mice infected with *Salmonella ΔAroA* (200 CFU). *N*=8 mice per group. Mean and SEM are shown. *P<0.05, ^{ns}P>0.05=not significant.

(B) WT, *Casp1/11*$^{-/-}$ and *Casp1/11/12*$^{-/-}$ BMDMs were infected with *Salmonella* SL1344 (MOI=50) and phosphorylation of MLKL analysed by Western blotting at the indicated timepoints. Probing for ß-actin served as a loading control.

Combined Loss of Caspase-1/11/12 and Caspase-8 Prevents *Salmonella* Induced Killing of BMDMs

Previous reports suggest that caspase-8 can induce pyroptotic cell death through cleavage of GSDMD (Mascarenhas et al., 2017). To explore the nature of the cell death induced by caspase-8 upon infection in cells lacking pyroptotic initiators, we used bone marrow-derived macrophages (BMDM) deficient for caspases-1/11 or caspases-1/11/12 and infected them with *Salmonella*. As previously reported, *Casp1/11*$^{-/-}$ BMDMs were protected from *Salmonella*-induced killing at very early time points (Franchi et al., 2006; Mariathasan et al., 2004). However, 6 h after infection with *Salmonella* a substantial fraction of *Casp1/11*$^{-/-}$ and also *Casp1/11/12*$^{-/-}$ BMDMs had died (Figure 2A). This reiterates that caspase-12 is not critical for the response to *Salmonella* infection. The delayed type of *Salmonella*-induced cell death in *Casp1/11*$^{-/-}$ and *Casp1/11/12*$^{-/-}$ BMDMs was unlikely to be due to necroptosis, as we could not detect changes in phosphorylation of MLKL, which are hallmarks of necroptosis (Figure S1B). Instead, *Casp1/11*$^{-/-}$ *and Casp1/11/12*$^{-/-}$ BMDMs displayed classical features of apoptosis, including cleavage of PARP as well as caspases-3, -7, -8 and -9 (Figure 2B), which extends a previous report showing that anthrax lethal toxin can induce a NLRP1-dependent form of cell death with comparable features of apoptosis in cells lacking caspase-1 (Van Opdenbosch et al., 2017). Lattice light sheet microscopy revealed nuclear condensation and plasma membrane blebbing. This is consistent with apoptotic death of *Salmonella*-infected *Casp1/11/12*$^{-/-}$ BMDMs and is in striking contrast to the pyroptotic death observed in *Salmonella*-infected WT BMDMs (Figure 2C and Suppl. Movies 1-3). Notably, combined loss of caspase-8 plus RIPK3 did not impair *Salmonella*-induced cell killing, as *in vitro* infected *Casp8/Ripk3*$^{-/-}$ BMDMs died with kinetics that were indistinguishable from WT cells, with both undergoing pyroptosis (Figure 2A). This is consistent with the observation that the combined loss of caspase-8 and RIPK3 did not impair bacterial control *in viv*o until at least 3

weeks post-infection (Figure 1B). These findings indicate that although caspase-8 was dispensable for the early pyroptotic cell death upon *Salmonella* infection, caspase-8 driven apoptosis rather than caspase-8 mediated pyroptosis or RIPK3/MLKL-driven necroptosis was responsible for the delayed type of cell death observed in *Casp1/11/12*$^{-/-}$ BMDMs. Strikingly, BMDMs from *Casp1/11/12/8/Ripk3*$^{-/-}$ mice that are unable to undergo pyroptosis, necroptosis and caspase-8 driven apoptosis were not only fully resistant to *Salmonella*-induced killing *in vitro* (Figure 2A), but also contained large numbers of bacteria (Figure 2C). This remarkable resistance to *Salmonella*-induced killing was not due to a general defect in cell death, as *Casp1/11/12/8/Ripk3*$^{-/-}$ BMDMs could still be killed through the intrinsic pathway of apoptosis by treatment with BH3 mimetic drugs, as shown by LDH release and activation of the apoptosis effector BAX (Figure S2A,B). Collectively, these findings uncover an intriguing back-up system that enables the host to flexibly deploy different types of programmed cell death for the control of the intracellular pathogen *Salmonella*.

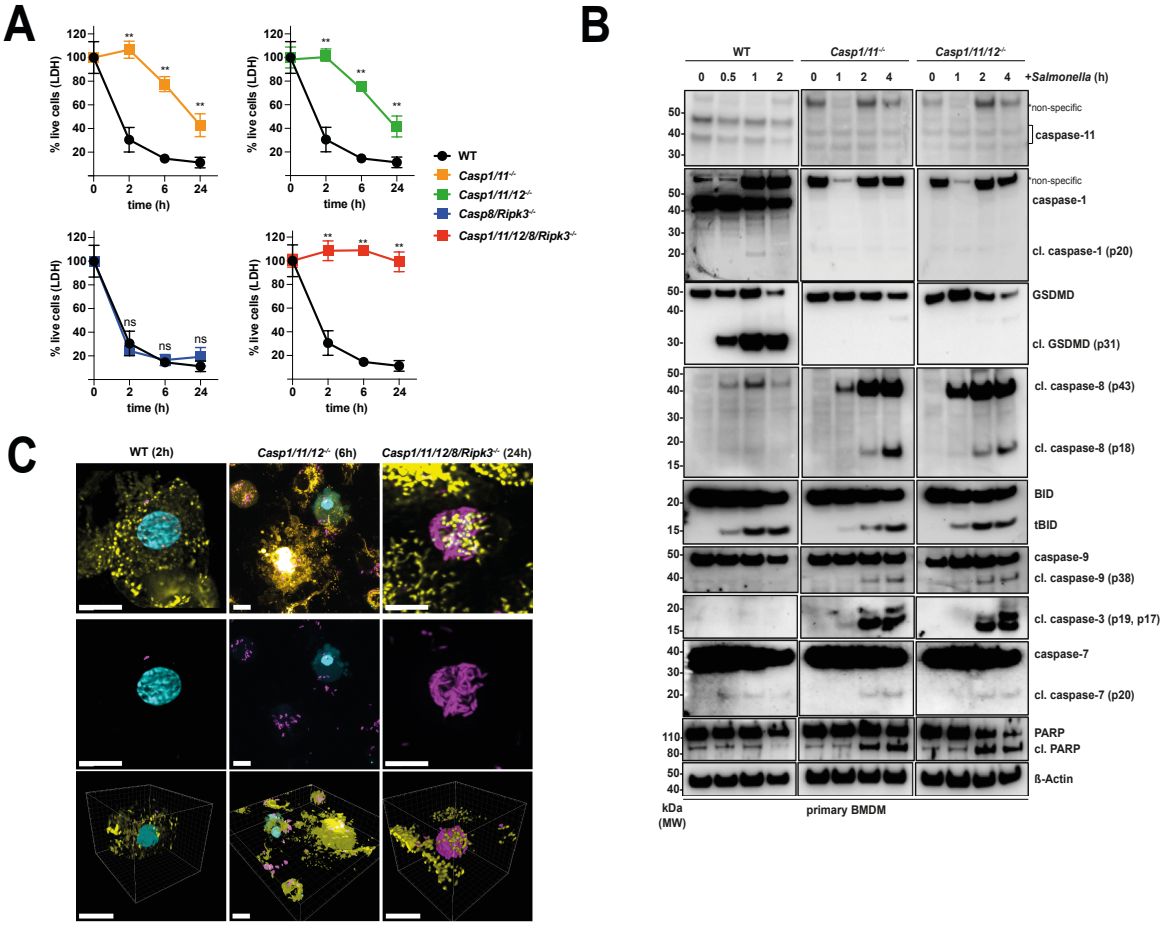

Figure 2. Combined Loss of Caspases-1/11/12 and Caspase-8 Abrogates the Death of BMDMs upon *Salmonella* Infection.

(A) LDH release cell death assay of WT, *Casp1/11*$^{-/-}$, *Casp1/11/12*$^{-/-}$, *Casp8/Ripk3*$^{-/-}$ and *Casp1/11/12/8/Ripk3*$^{-/-}$ primary BMDMs infected with *Salmonella* SL1344 (MOI=50). Data pooled from 2 or more experiments. Mean and SEM are shown. **P<0.005; ^{ns}P>0.05=not significant.

(B) WT, *Casp1/11*$^{-/-}$ and *Casp1/11/12*$^{-/-}$ BMDMs were infected with *Salmonella* SL1344 (MOI=50) and cleavage/activation of the indicated cell death regulators were analyzed by Western blotting at the indicated time points. Probing for ß-actin served as a loading control.

(C) Confocal or lattice light sheet imaging of WT, *Casp1/11/12*$^{-/-}$ or *Casp1/11/12/8/Ripk3*$^{-/-}$ primary BMDMs infected with *Salmonella* SPi-2 (GFP) (MOI=50) at the indicated time points. Yellow - Membranes, Magenta – *Salmonella*, Cyan – PI. Scale bars: 10 µm.

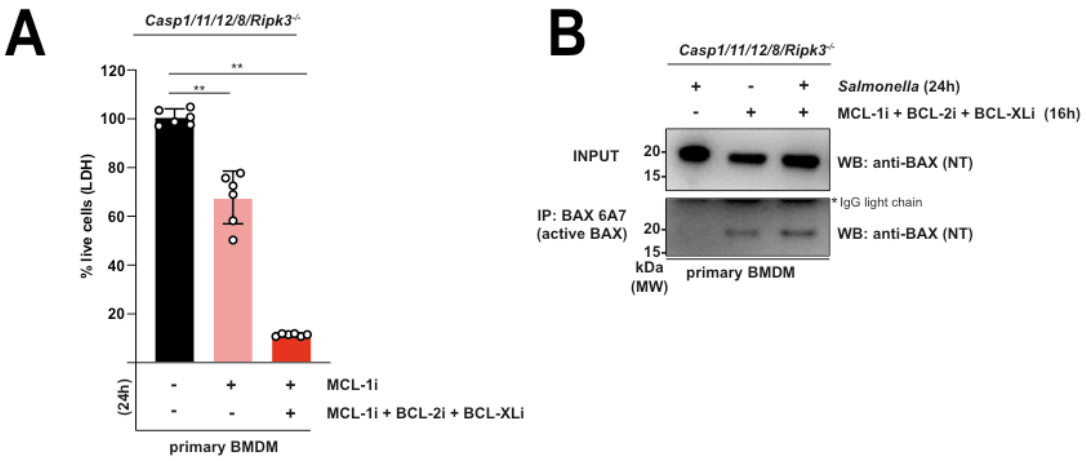

Figure S2. Primary BMDMs from *Casp1/11/12/8/Ripk3*$^{-/-}$ Mice Are Susceptible to Intrinsic Apoptosis Induced by BH3 Mimetic Drugs.

(A) *Casp1/11/12/8/Ripk3*$^{-/-}$ BMDMs were treated with BH3 mimetic drugs individually (2 µM MCL1i) or in combination (each 2 µM of MCL1i + BCL2i + BCL-XLi) as indicated. Cell death was measured using an LDH release assay. Data pooled from 2 or more experiments. Mean and SD are shown. **P<0.005.

(B) Immunoprecipitation and immunoblotting of activated BAX in *Casp1/11/12/8/Ripk3*$^{-/-}$ BMDMs infected with *Salmonella* SL1344 (MOI=50) and/or treated with BH3 mimetic drug combination (each 2 µM of MCL1i + BCL2i + BCL-XLi).

Immortalized BMDMs facilitate unravelling of the diverse cell death mechanisms induced upon *Salmonella* infection.

To gain a deeper understanding of this complex system of functional backup between different cell death processes, we used our CRISPR/Cas9 gene knockout platform (Aubrey et al., 2015) to identify the initiators and effectors that are critical for driving the respective types of cell death upon *Salmonella* infection *in vitro*. We used immortalized BMDMs (iBMDMs) for these experiments, which exhibited comparable responses to *Salmonella* infection as primary BMDMs (Figure 3A,B). While the combined loss of caspases-1/11/12 delayed *Salmonella*-induced killing of iBMDMs, the combined deletion of caspase-8 and RIPK3 had no impact and cells died in a manner comparable to WT cells (Figure 3A). Only the combined deletion of caspases-1/11/12 plus caspase-8/RIPK3 was able to completely block *Salmonella* infection induced killing of iBMDMs (Figure 3A). To test whether the genetically manipulated *Casp1/11/12/8/Ripk3*^{KO} iBMDMs were completely unable to undergo cell death as was the case for primary BMDMs (Figure S2A,B), we treated them with combinations of BH3 mimetics or etoposide (Figure S3A,B). These treatments resulted in efficient killing of the *Casp1/11/12/8/Ripk3*^{KO} iBMDMs, accompanied by activation of the apoptosis effector BAX (Figure S3A,B).

Interestingly we noted that in the absence of caspases-1/11/12, infection of iBMDMs with *Salmonella* led to a strong induction of caspase-8 and caused the appearance of classical markers of apoptosis, such as cleaved BID, caspases-3, -7 and -9 (Figure 3B). *Casp1/11/12*^{KO} cells infected with *Salmonella* in the absence or presence of the highly selective RIPK1 inhibitor, Nec1s (Figure 3C, D) still underwent cell death and activated caspase-8, BID and caspase-3. As Nec1s blocked necroptosis induced by a combination of TNF-α+Birinipant+Emricasan in control experiments (Figure S4A), these findings indicate that the activation of caspase-8 under these conditions was unlikely to be caused by the ripoptosome

(Tenev et al., 2011). Collectively, these results validate iBMDMs as useful tools to unravel the molecular requirements of the diverse cell death pathways induced upon *Salmonella* infection.

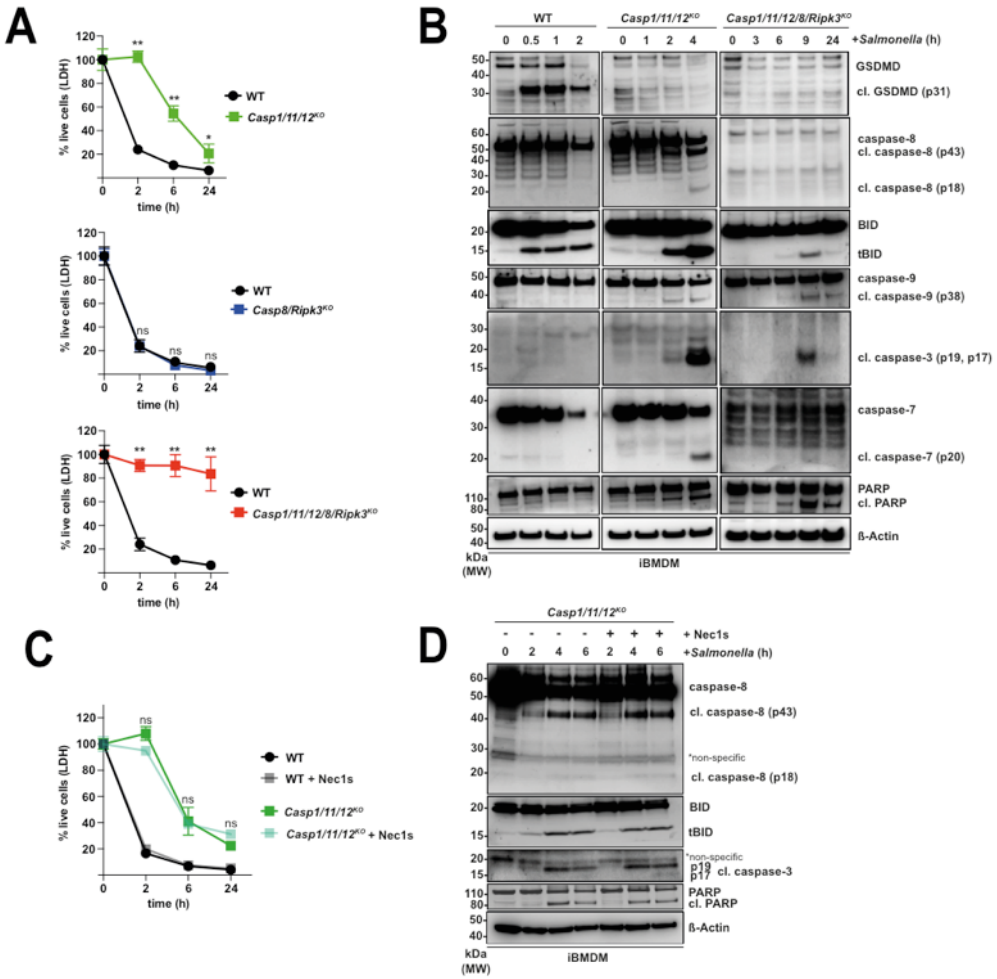

Figure 3. Caspase-8-Mediated Apoptosis Is the Default Backup Mechanism when Caspase1/11-Mediated Pyroptosis Is Disabled in Salmonella infected iBMDMs.
(A) LDH release cell death assay of WT, *Casp1/11/12*^{KO}, *Casp8/Ripk3*^{KO} and *Casp1/11/12/8/Ripk3*^{KO} iBMDMs infected with *Salmonella* SL1344 (MOI=50). Data pooled from 2 or more experiments. Mean and SEM are shown. **P<0.005; ^{ns}P>0.05=not significant.
(B) Western blot analysis of the indicated proteins in WT, *Casp1/11/12*^{KO} and *Casp1/11/12/8/R3*^{KO} iBMDMs infected with *Salmonella* SL1344 (MOI=50). Probing for ß-actin served as a loading control.
(C) LDH release cell death assay of *Salmonella* SL1344 (MOI=50) infected WT and *Casp1/11/12*^{KO} iBMDMs that had been left untreated or treated with the RIPK1 inhibitor, Nec1s (30 µM). Data pooled from 2 or more experiments. Mean and SEM are shown. **P<0.005; ^{ns}P>0.05=not significant.
(D) Western blot analysis of *Salmonella* SL1344 (MOI=50) infected WT and *Casp1/11/12*^{KO} iBMDMs that had been left untreated or treated with the RIPK1 inhibitor, Nec1s (30 µM). Probing for ß-actin served as a loading control.

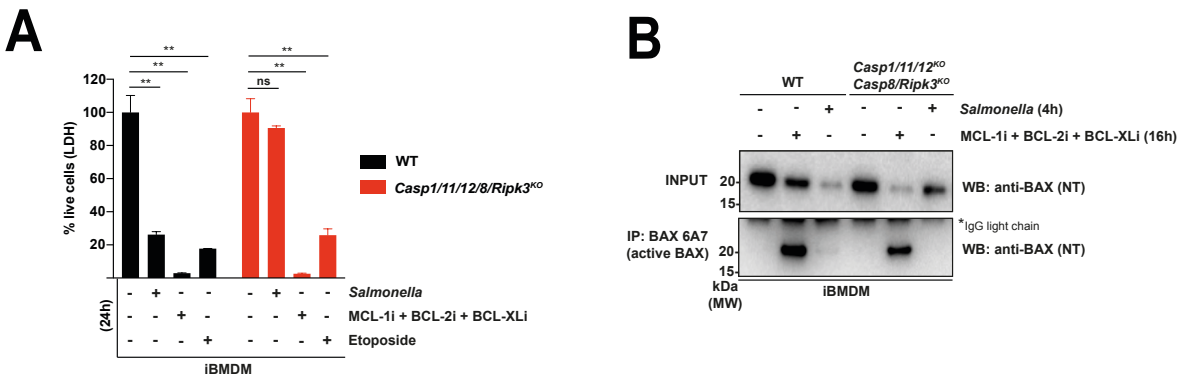

Figure S3. *Casp1/11/12/8/Ripk3*^{KO} iBMDMs Are Susceptible to Intrinsic Apoptosis Induced by BH3 Mimetic Drugs

(A) LDH release cell death assay of WT and *Casp1/11/12/8/Ripk3*^{KO} iBMDMs after 24 h treatment with combination of BH3 mimetic drugs (each 2 µM of MCL1i + BCL-2i + BCL-XLi), Etoposide (50 µM) or infection with *Salmonella* SL1344 (MOI=50). Mean and SEM are shown. **P<0.005; ^{ns}P>0.05=not significant.

(B) Immunoprecipitation and immunoblotting of activated BAX in WT and *Casp1/11/12/8/Ripk3*^{KO} iBMDMs infected with *Salmonella* SL1344 (MOI=50) or treated with BH3 mimetic drug combination (each 2 µM of MCL-1i + BCL2i + BCL-XLi).

Caspase-11 can partially compensate for the loss of caspase-1 and caspase-8 by triggering GSDMD-dependent death of *Salmonella* infected cells

To identify which of the initiator caspases-1, -11, -12 or -8 are necessary for induction of cell death in *Salmonella*-infected cells, we treated WT, *Casp1/11/12*^{KO} and *Casp8/Ripk3*^{KO} iBMDMs with different caspase inhibitors and examined the cell death response (Figure 4A and Figure S4B). Surprisingly, the pan-caspase inhibitor Emricasan could stalled the early cell death response as observed in *Casp1/11/12*$^{-/-}$ BMDMs, but did not prevent the subsequent cell death induced upon *Salmonella* infection in WT cells (Figure 4A). We hypothesised that this was due to necroptosis following blockade of caspase-8, which we confirmed by the induction of cell death in WT but not MLKL-deficient cells treated with Emricasan (Figure S4B). Accordingly, we could completely block the killing of *Salmonella*-infected *MLKL*^{KO} iBMDMs by treatment with Emricasan (Figure 4A), clearly demonstrating that caspase activity is required for *Salmonella*-induced cell killing. As expected, caspase-1 inhibition by VX765 delayed but did not affect the overall survival of *Salmonella* infected WT, *MLKL*^{KO} and *Casp1/11/12*^{KO} cells (Figure S4A and 4A). These findings not only validate the above observations through pharmacological approaches, but also indicate that the phenomena described so far are not the consequence of longer-term adaptations caused by the loss of the genes of interest.

Notably, inhibition of caspase-1 activity using VX765 or genetic deletion of caspase-1 in *Casp8/Ripk3*^{KO} iBMDMs did not fully recapitulate the striking survival of *Salmonella*-infected *Casp1/11/12/8/Ripk3*^{KO} iBMDMs although it delayed their killing (Figure 4A & B). We therefore surmised that caspase-11 provided a back-up mechanism for cell killing when caspase-1 and caspase-8 were absent or inhibited (Man et al., 2017; Ng and Monack, 2013). To investigate this, we generated *Casp1/11/8/Ripk3*^{KO} iBMDMs and compared their death kinetics to those of *Casp1/11/12/8/Ripk3*^{KO} cells. *Casp1/8/Ripk3*^{KO} iBMDMs responded to the

403 infection by upregulation of caspase-11 and cell killing, although it was noteworthy that cell
404 death was less effective with ~60-70% of the cells surviving the bacterial assault (Figure 4B,
405 D). *Casp1/11/8/Ripk3*^{KO} phenocopied *Casp1/11/12/8/Ripk3*^{KO} cells in that they were fully
406 resistant to *Salmonella*-induced death (Figure 4B), once again underlining the redundancy of
407 caspase-12 for cell death during infection with this intracellular pathogen (Figure 4B). The
408 pan-caspase inhibitor Emricasan completely blocked the cell death in *Salmonella*-infected
409 *Casp1/8/Ripk3*^{KO} iBMDMs and we could no longer detect activated forms of GSDMD, the
410 critical effector of pyroptosis (Figure 4 C, D). Notably, infection of *Casp1/8/Ripk3*^{KO} iBMDMs
411 with *Salmonella* did not result in the occurrence of apoptotic markers, such as cleaved BID or
412 PARP (Figure 4D), and the additional deletion of GSDMD rendered *Casp1/8/Ripk3*^{KO}
413 iBMDMs fully resistant to *Salmonella*-induced killing (Figure 4C). Thus, although caspase-11
414 can kill some *Salmonella* infected cells in the absence of caspase-1 and caspase-8, the
415 protracted kinetics and exclusive dependence on GSDMD suggest a comparatively minor role
416 for caspase-11 in the 'back-up' system governing *Salmonella* induced killing.
417
418
419
420
421
422
423
424

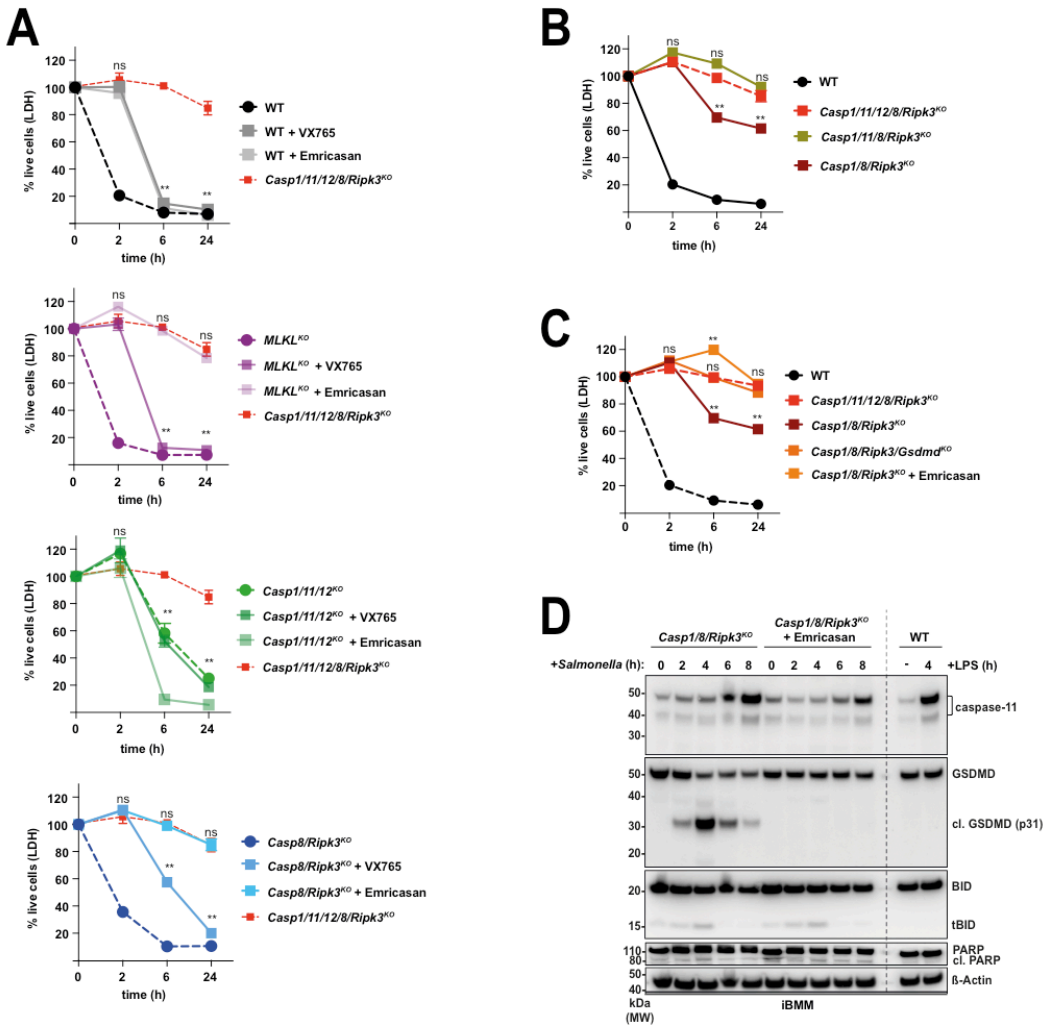

Figure 4: Caspase-11 Can Compensate for the Loss of Caspase-1 and Caspase-8 to Ensure GsdmD-Mediated Killing of *Salmonella* Infected Cells.

(A) LDH release cell death assay of *Salmonella* SL1344 (MOI=50) infected WT, $MLKL^{KO}$, $Casp1/11/12^{KO}$, $Casp8/Ripk3^{KO}$ and $Casp1/11/12/8/Ripk3^{KO}$ iBMDMs that had been left untreated or treated with VX-765 or Emricasan. Data pooled from 2 or more experiments. Mean and SEM are shown. **P<0.005; ^{ns}P>0.05=not significant.

(B) LDH release cell death assay of WT, $Casp1/8/Ripk3^{KO}$, $Casp1/11/8/Ripk3^{KO}$ and $Casp1/11/12/8/Ripk3^{KO}$ iBMDMs that had been infected with *Salmonella* SL1344 (MOI=50). Data pooled from 2 or more experiments. Mean and SEM are shown. **P<0.005; ^{ns}P>0.05=not significant.

(C) LDH release cell death assay of WT, $Casp1/8/Ripk3^{KO}$, $Casp1/8/Ripk3/Gsdmd^{KO}$ and $Casp1/11/12/8/Ripk3^{KO}$ iBMDMs or $Casp1/8/Ripk3^{KO}$ that had been left untreated or treated with Emricasan that had been infected with *Salmonella* SL1344 (MOI=50). Data pooled from 2 or more experiments. Mean and SEM are shown. **P<0.005; ^{ns}P>0.05=not significant.

(D) Western blot analysis of caspase-11, GSDMD, BID and PARP in $Casp1/8/R3^{KO}$ iBMDMs that had been left untreated or treated with Emricasan that had been infected with *Salmonella* SL1344 (MOI=50). WT iBMDMs that had been left untreated or treated with LPS for 4h were used as control for caspase-11 induction. Probing for ß-actin served as a loading control.

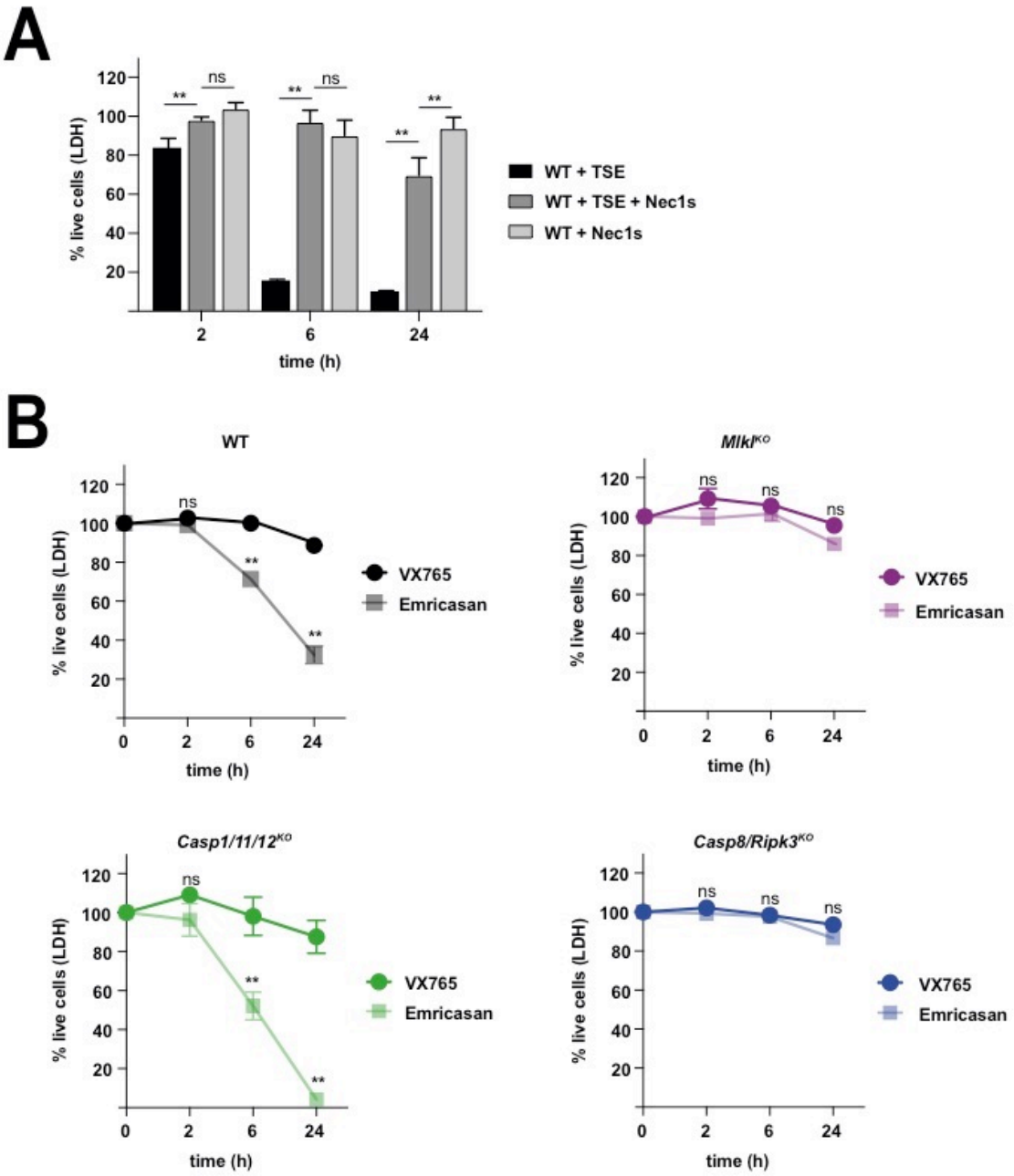

Figure S4: Impact of RIPK1 Inhibition by Nec1s and Effect of Caspase-1 Inhibition or Inhibition of All Caspases on the Survival of iBMDM.

(A) WT iBMDMs were treated with TNF-α (100 ng/mL) + Birinapant (1 μM) + Emricasan (20 μM) with or without the RIPK1 inhibitor Nec1s (30 μM) and cell death was measured by LDH release. Data pooled from 2 or more experiments. Mean and SEM are shown. **P<0.005; ^{ns}P>0.05=not significant.

(B) LDH release cell death assay of WT, *MLKL^{KO}, Casp1/11/12^{KO}, Casp1/11/12/MLKL^{KO}*, *Casp8/Ripk3^{KO}* and *Casp1/11/12/8/Ripk3^{KO}* iBMDMs that had been treated with the caspase-1 specific inhibitor, VX-765 (20 μM), or the broad-spectrum caspase inhibitor, Emricasan (20 μM). Data pooled from 2 or more experiments. Mean and SEM are shown. **P<0.005; ^{ns}P>0.05=not significant.

Caspase-1 orchestrates a wide range of diverse cell death inducing processes with remarkable plasticity

Although our data show an important role for caspase-8 in compensating for the lack of pyroptosis (in mice lacking caspases-1/11/12), it was also evident that host defense was intact in mice lacking both caspase-8 and RIPK3 (Figure 1B). This suggests that there may not only be redundancy amongst the different cell death pathways, but that individual components of these processes could possibly be employed in more than one pathway. With this in mind, we reasoned that the lack of caspase-8-mediated apoptosis might be compensated for by caspase-1. To investigate this, we deleted GSDMD to prevent caspase-1 and caspase-11 from triggering pyroptosis and also eliminated caspase-8 and RIPK3 from iBMDMs. Intriguingly, cells lacking these essential components of apoptosis and necroptosis as well as being unable to execute pyroptosis still died upon *Salmonella* infection with kinetics that were indistinguishable from *Gsdmd*^{KO} iBMDMs (Figure 5A). We noted that *Salmonella*-infected *Gsdmd/Casp8/Ripk3*^{KO} iBMDMs not only had active caspase-1, as predicted, but also contained cleaved BID (tBID) and cleaved caspases-3, -7 and -9 (Figure 5B). This indicates that caspase-1 may trigger caspase-8-independent apoptosis via BID-driven, BAX/BAK-mediated MOMP and the resulting activation of caspase-9, thereby stimulating the effector caspases-3 and -7. This is consistent with recent reports (Heilig et al., 2020; Tsuchiya et al., 2019) and suggests that caspase-1 can induce apoptosis by bypassing caspase-8 through the mitochondrial amplification loop. Intriguingly, preventing MOMP through the combined deletion of BAX and BAK in *Gsdmd/Casp8/Ripk3*^{KO} iBMDMs did not have the expected effect of blocking *Salmonella* induced cell killing; instead, *Gsdmd/Casp8/Ripk3/Bax/Bak*^{KO} iBMDMs still died upon *Salmonella* infection containing active caspases-3 and -7 (Figure 5A,B). This indicates that the absence of BAX/BAK could be compensated for by rewiring the cell in a manner that allows for caspase-1 to trigger the executioner caspases (caspases-3 and -7) independently of

MOMP. Surprisingly, ablating this alternative cell death circuit by deleting caspases-3 and -7 was yet again not sufficient to prevent cell death, as *Gsdmd/Casp8/Ripk3/Casp3/7*^{KO} iBMDMs still died upon *Salmonella* infection, although this occurred with slower kinetics compared to *Gsdmd/Casp8/Ripk3/Bax/Bak*^{KO} iBMDMs (Figure 5C). The fact that *Gsdmd/Casp8/Ripk3/Casp3/7*^{KO} iBMDMs still contained cleaved BID (tBID) and cleaved caspases-1 and -9 suggested that tBID and caspase-9 activated by caspase-1 could overcome the lack of the executioner caspases to ensure killing of infected cells (Figure 5D). Intriguingly, additional deletion of BID from *Gsdmd/Casp8/Ripk3/Casp3/6/7*^{KO} iBMDMs did not render the cells fully resistant to *Salmonella*-induced death. This raised the exciting prospect that caspase-1 can directly activate caspase-9, which then acted as an effector caspase rather than an initiator caspase (Figure 5E). Of note, the deletion of caspase-9 from *Gsdmd/Casp8/Ripk3/Bid/Mlkl/Casp3/7*^{KO} iBMDMs finally reproduced the profound resistance to *Salmonella*-induced cell killing observed in *Casp1/11/12/8/Ripk3*^{KO} iBMDMs (Figure 5F). These findings reveal a remarkable degree of plasticity with which caspase-1 can orchestrate the use of diverse cell death-inducing processes to kill *Salmonella* infected iBMDMs. Caspase-1 can bypass caspase-8 by initiating apoptosis through mitochondrial amplification and can even circumvent the need for MOMP by activating caspases-3, -7 or -9 directly (see schematic in Figure 5G). This shows that many core components widely believed to be essential for apoptosis can be bypassed and that the resulting re-routing of the cell death machinery provides various alternative processes for the killing of pathogen infected cells.

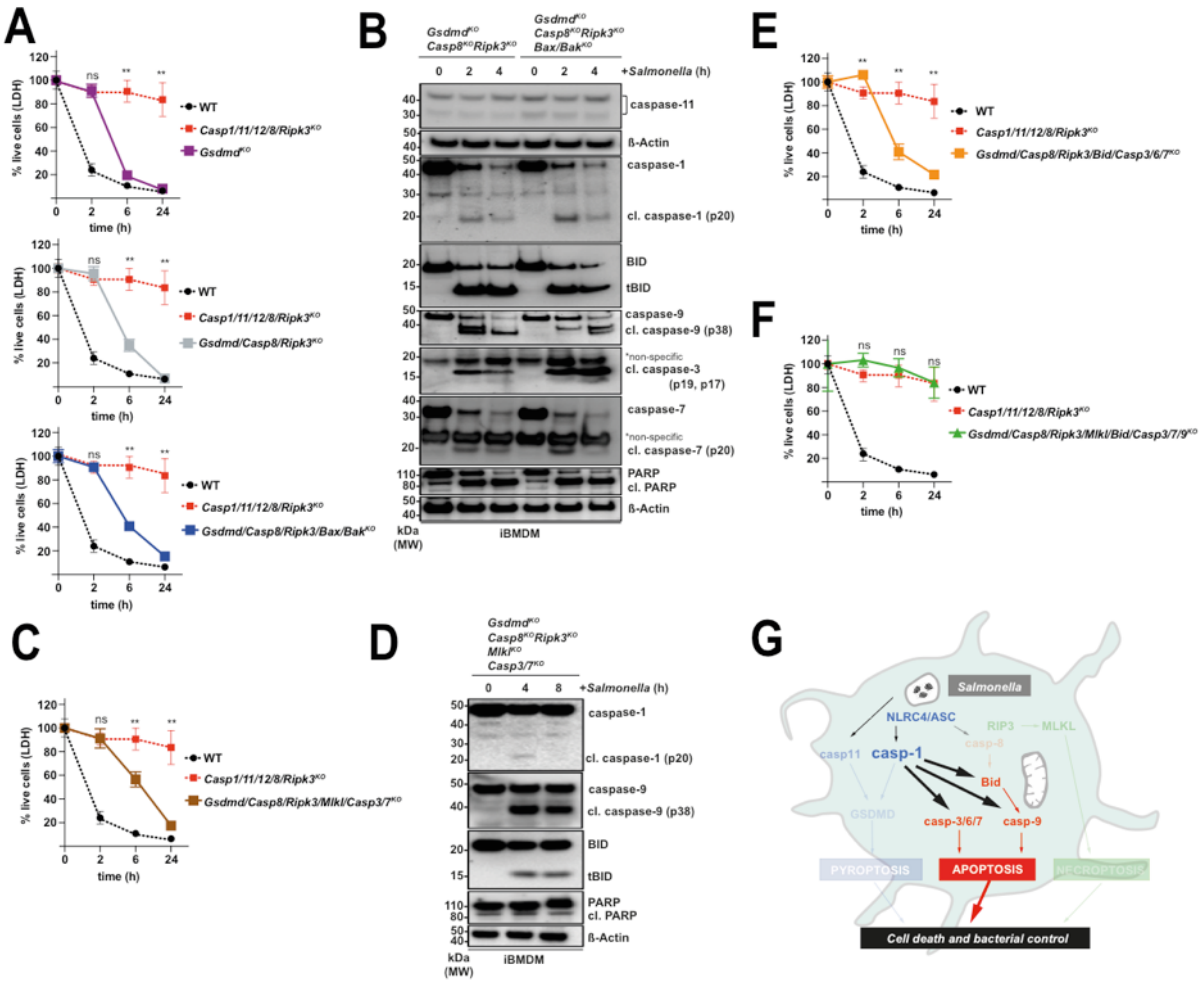

507

508 **Figure 5. Caspase-1 Can Activate Caspases-3, -7 and -9 Independently of Caspase-8 and**
509 **BID.**
510 **(A)** LDH release cell death assay of WT, *Casp1/11/12/8/Ripk3*^{KO}, *GsdmD*^{KO},
511 *GsdmD/Casp8/Ripk3*^{KO} and *GsdmD/Casp8/Ripk3/Bax/Bak*^{KO} iBMDMs that had been infected
512 with *Salmonella* SL1344 (MOI=50). Data pooled from 2 or more experiments. Mean and SEM
513 are shown. **P<0.005; ^{ns}P>0.05=not significant.
514 **(B)** *GsdmD/Casp8/Ripk3*^{KO} and *GsdmD/Casp8/Ripk3/Bax/Bak*^{KO} iBMDMs were infected with
515 *Salmonella* SL1344 (MOI=50) and cleavage/activation of the indicated cell death proteins was
516 analyzed by Western blotting at the indicated time points. Probing for ß-actin served as a
517 loading control.
518 **(C)** LDH release cell death assay of WT, *Casp1/11/12/8/Ripk3*^{KO} and
519 *GsdmD/Casp8/Ripk3/Mlkl/Casp3/7*^{KO} iBMDMs that had been infected with *Salmonella*
520 SL1344 (MOI=50). Data pooled from 2 or more experiments. Mean and SEM are shown.
521 **P<0.005; ^{ns}P>0.05=not significant.
522 **(D)** *GsdmD/Casp8/Ripk3/Mlkl/Casp3/7*^{KO} iBMDMs were infected with *Samonella* SL1344
523 (MOI=50) and expression and cleavage/activation of the indicated cell death proteins was
524 analyzed by Western blotting at the indicated time points. Probing for ß-actin served as a
525 loading control.
526 **(E)** LDH release cell death assay of WT, *Casp1/11/12/8/Ripk3*^{KO} and
527 *GsdmD/Casp8/Ripk3/Bid/Casp3/7*^{KO} iBMDMs that had been infected with *Salmonella* SL1344
528 (MOI=50). Data pooled from 2 or more experiments. Mean and SEM are shown. ^{ns}P>0.05=not
529 significant.

(F) LDH release cell death assay of WT, *Casp1/11/12/8/Ripk3*^{KO} and *GsdmD/Casp8/Ripk3/Mlkl/Bid/Casp3/7/9*^{KO} iBMDMs that had been infected with *Salmonella* SL1344 (MOI=50). Data pooled from 2 or more experiments. Mean and SEM are shown. ^{ns}P>0.05=not significant.
(G) Schematic overview of cell death induction by caspase-1 in the absence of pyroptosis and caspase-8.

Caspase-1 has a central role as both a cell death inducer and executioner

Our findings provided intriguing insights into the role of caspase-1 and its capacity to compensate for the lack of caspase-8. However, it is important to note that *Casp1/11*$^{-/-}$ and *Casp1/11/12*$^{-/-}$ mice nonetheless effectively controlled *Salmonella* infection (Figure 1B). This highlights yet another form of compensation whereby caspase-1 can also be functionally replaced. This likely involved caspase-8, as suggested by the observations that *Casp1/11/12/8/Ripk3*$^{-/-}$ mice were unable to clear bacteria and that BMDMs derived from these animals failed to undergo cell death upon infection (Figures 1B,C). We therefore tested the hypothesis that deleting the death effectors regulated by caspases-1 and -8, i.e. GSDMD/BID/MLKL/caspase-3/6/7, and possibly also caspase-9, would recapitulate the profound resistance to *Salmonella*-induced killing observed in *Casp1/11/12/8/Ripk3*^{KO} iBMDMs. However, upon infection with *Salmonella* both *Gsdmd/Bid/Mlkl/Casp3/7/9*^{KO} and *Gsdmd/Bid/Mlkl/Casp3/6/7/9*^{KO} iBMDMs underwent substantial cell death, although this was delayed compared to WT iBMDMs (Figure 6A). To identify the most potent upstream regulator(s) of this unexpected cell killing caused by *Salmonella*, we performed a genome-wide CRISPR/Cas9 knockout screen (Figure S5A). We transduced Cas9 expressing *Gsdmd/Bid/Mlkl/Casp3/7/9*^{KO} iBMDMs with a whole genome sgRNA library (Koike-Yusa et al., 2014) and stringently enriched for sgRNAs that promoted cell survival after *Salmonella* infection by repeating the infection/selection procedure three times. Amplicon sequencing of the sgRNAs enriched in the surviving cells identified caspase-1 and its activator NLRC4 (Figures 6B and S5B).

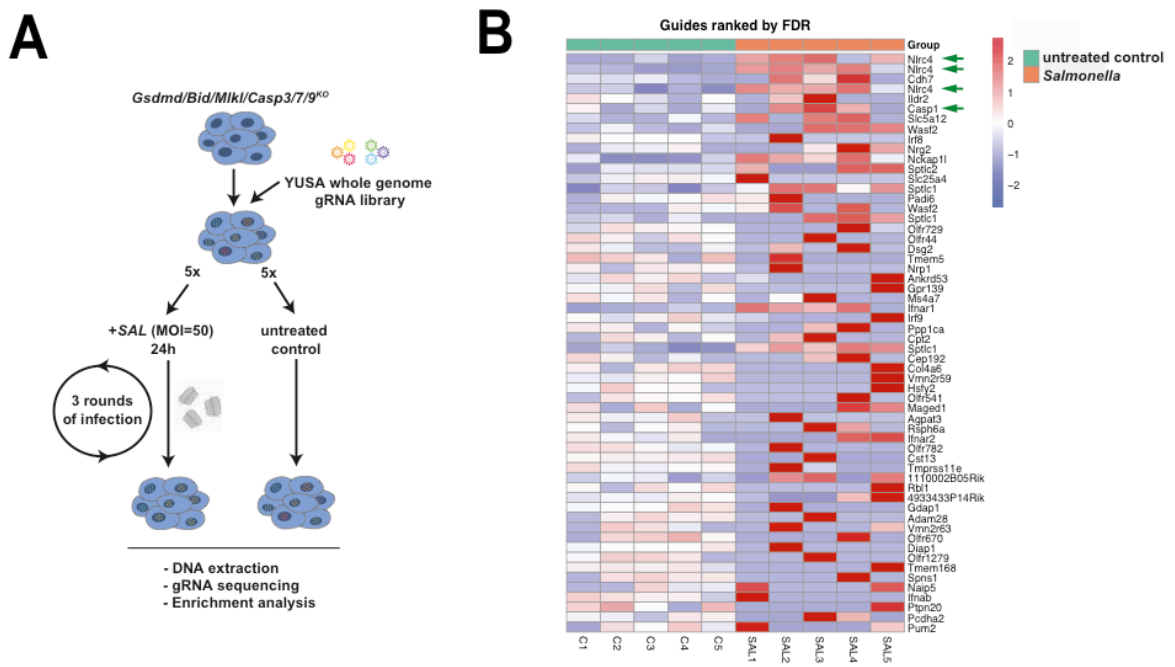

Figure S5. CRISPR/Cas9 Screen Identifies Caspase-1 and NRLC4 as the Central Drivers of Cell Death in the Absence of all known Downstream Effectors of Cell Killing.
(A) Schematic overview of CRISPR/Cas9 whole genome screen: *Gsdmd/Bid/Mlkl/Casp3/7/9*^{KO} iBMDMs were transduced with a whole genome sgRNA library (Koike-Yusa et al., 2014) and infected in replicates for three consecutive rounds with *Salmonella* SL1344 (MOI=50). Surviving cells were expanded and subjected to NGS analysis. **(B)** A heatmap of the sgRNAs significantly enriched during the CRISPR/Cas9 screen as shown per individual replicate, ranked according to false discovery rate. Green arrowheads indicate sgRNAs for caspase-1 and NLRC4.

571 This raised the possibility that the initiator caspase-1 can kill *Salmonella*-infected iBMDMs
572 directly (i.e. acting not only as an initiator but also as an effector caspase), which would also
573 explain why cells still died in the absence of pore formation (GSDMD) and all other effectors
574 that are known to function downstream of caspase-1. Consistent with such a role for caspase-
575 1, Western blot analysis revealed processing of both caspase-1 and caspase-8 in *Salmonella*-
576 infected *Gsdmd/Bid/Mlkl/Casp3/7/9*^{KO} iBMDMs (Figure 6C). Deletion of caspase-1 in
577 *Gsdmd/Bid/Mlkl/Casp3/7/9*^{KO} iBMDMs rendered these cells fully resistant to *Salmonella*-
578 induced killing despite the presence of caspase-8, which was comparable to
579 *Casp1/11/12/8/Ripk3*^{KO} cells (Figure 6D). Together with our demonstration that
580 *Gsdmd/Bid/Mlkl/Casp3/7/9*^{KO} iBMDMs in which caspase-8 was deleted (Figure 5E) were also
581 fully resistant to *Salmonella*-induced death, these findings indicate that cell death under these
582 circumstances was only possible when both caspase-1 and caspase-8 were present.
583
584

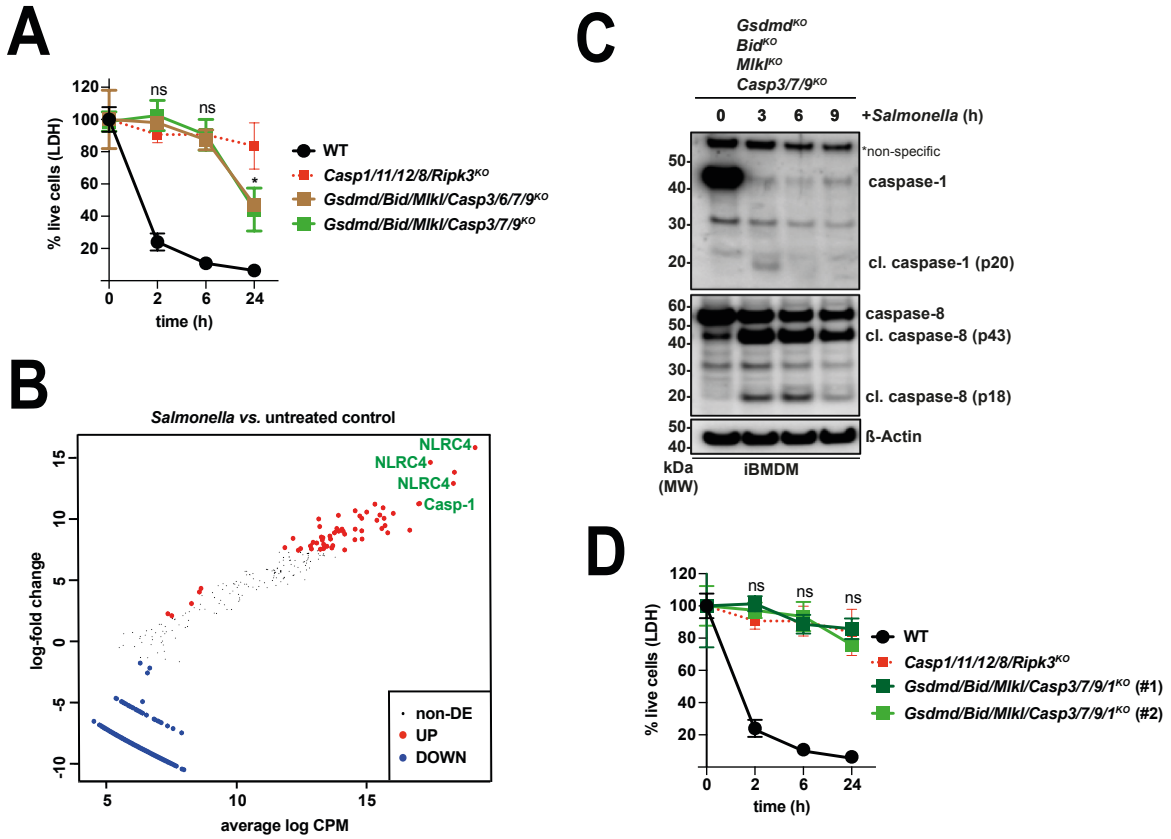

Figure 6. CRISPR Screen Reveals a Central Role for Caspase-1 in Mediating *Salmonella* Infection Induced Cell Death Independent of All Known Downstream Effectors of Cell Killing.

(A) LDH release cell death assay of WT, *Casp1/11/12/8/Ripk3*^{KO}, *GsdmD/Bid/Mlkl/Casp3/7/9*^{KO} and *GsdmD/Bid/Mlkl/Casp3/6/7/9*^{KO} iBMDMs that had been infected with *Salmonella* SL1344 (MOI=50). Data pooled from 2 or more experiments. Mean and SEM are shown. *P<0.05; ^{ns}P>0.05=not significant.

(B) *GsdmD/Bid/Mlkl/Casp3/7/9*^{KO} whole genome CRISPR/Cas9 screen mean-difference (MD) plot showing log-fold change *vs* Average log counts per million (CPM) after 3 rounds of infection with *Salmonella* SL1344 (MOI=50) (see Suppl Fig. 5A).

(C) *GsdmD/Bid/Mlkl/Casp3/7/9*^{KO} iBMDMs were infected with *Salmonella* SL1344 (MOI=50) and cleavage/activation of caspase-1 and caspase-8 was analyzed by Western blotting at the indicated time points. Probing for β-actin served as a loading control.

(D) LDH release cell death assay of WT, *Casp1/11/12/8/Ripk3*^{KO} and two independent clones (#1; #2) of *GsdmD/Bid/Mlkl/Casp3/7/9/1*^{KO} iBMDMs that had been infected with *Salmonella* SL1344 (MOI=50). Data pooled from 2 or more experiments. Mean and SEM are shown. ^{ns}P>0.05=not significant.

606 **Caspase-1 acts upstream of and requires caspase-8 to induce cell death in the absence of**
607 **all known downstream cell death effectors**
608 Interestingly, we found that the caspase-8 cleavage we had observed in
609 *Gsdmd/Bid/Mlkl/Casp3/6/7/9*^{KO} iBMDMs was strongly reduced in *Salmonella*-infected
610 *Gsdmd/Bid/Mlkl/Casp1/3/7/9*^{KO} iBMDMs (Figure 7A), indicating that caspase-1 was required
611 for full activation of caspase-8. This identifies caspase-1 as the most potent upstream initiator
612 of *Salmonella*-induced cell killing and explains why we only enriched for sgRNAs targeting
613 caspase-1 and its activator NLRC4 in the CRISPR screen. Supporting this idea, we found that
614 both the caspase inhibitor Emricasan and the highly specific caspase-1 inhibitor VX-765
615 completely blocked *Salmonella*-induced killing of *Gsdmd/Bid/Mlkl/Casp3/7/9*^{KO} iBMDMs
616 (Figure 7B). Furthermore, similar to the genetic deletion of *Caspase-1*, VX-765 almost
617 completely blocked caspase-8 processing in *Salmonella*-infected
618 *Gsdmd/Bid/Mlkl/Casp3/6/7/9*^{KO} cells (Figure 7C). Of note, this type of cell death that was
619 ensured as long as both caspase-1 and caspase-8 were present looked morphologically like
620 apoptosis as demonstrated by brightfield microscopy of *Salmonella*-infected
621 *Gsdmd/Bid/Mlkl/Casp3/7/9*^{KO} iBMDMs (Figure S6). These results show that *Salmonella*-
622 infected macrophages can undergo programmed cell death in the absence of all known effector
623 mechanisms of pyroptosis, apoptosis or necroptosis as long as caspase-1 and caspase-8 can be
624 activated (schematic shown in Figure 7D).
625

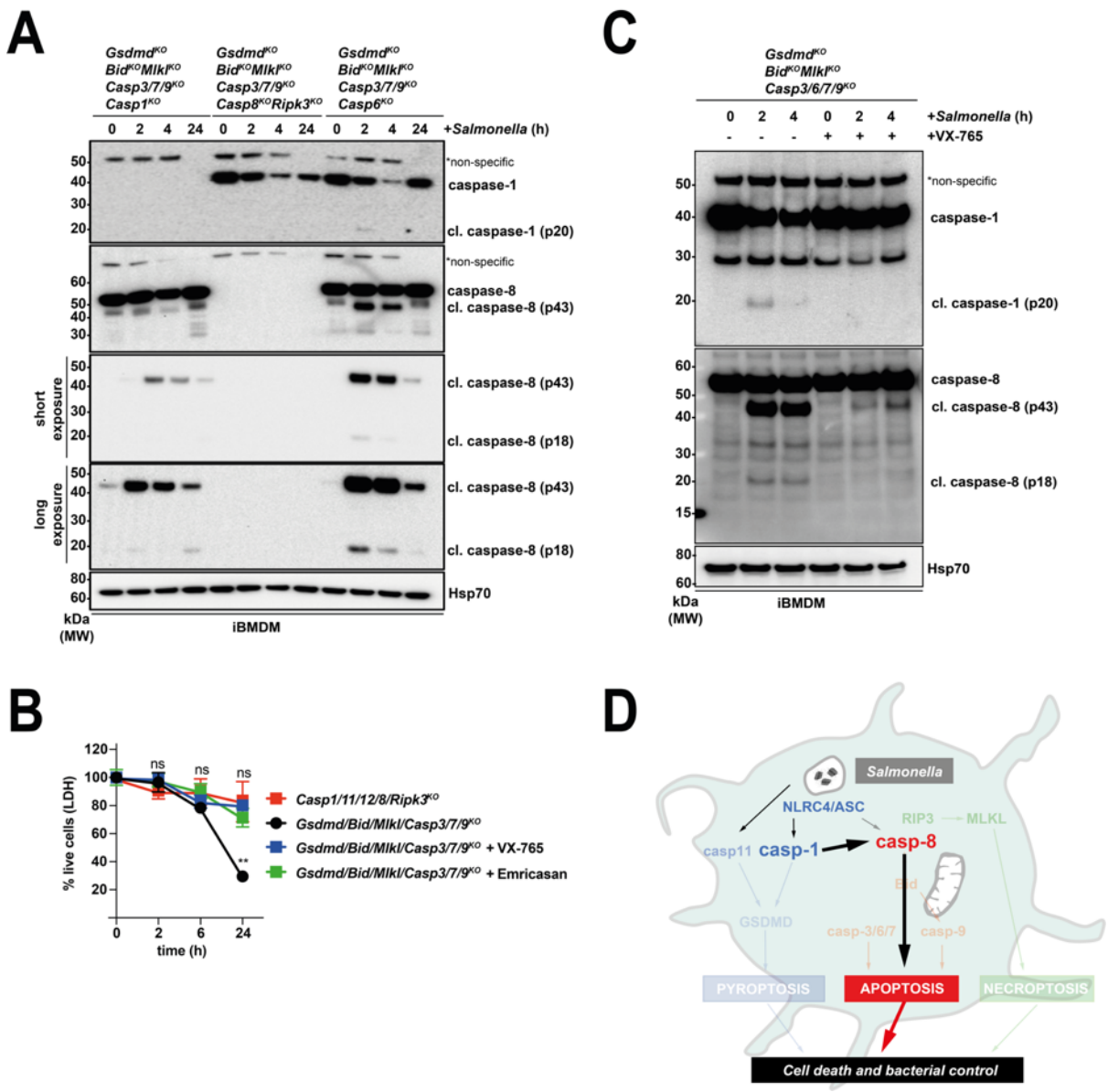

Figure 7. Caspase-1 Acts Upstream of and Requires Caspase-8 to Induce Cell Death in the Absence of All Known Downstream Effectors of Pyroptosis and Apoptosis.

(A) *GsdmD/Bid/Mlkl/Casp3/7/9/Casp1*^{KO}, *GsdmD/Bid/Mlkl/Casp3/7/9/Casp8/Ripk3*^{KO} and *GsdmD/Bid/Mlkl/Casp3/7/9/Casp6*^{KO} iBMDMs were infected with *Samonella* SL1344 (MOI=50) and cleavage/activation of caspase-1 and caspase-8 was analyzed by Western blotting at the indicated time points. Probing for HSP70 served as loading control.

(B) LDH release death assay of *Salmonella* SL1344 (MOI=50) infected *Casp1/11/12/8/Ripk3*^{KO} and *GsdmD/Bid/Mlkl/Casp3/7/9*^{KO} that had been left untreated or treated with VX-765 or Emricasan. Data pooled from 2 experiments. Mean and SEM are shown. **P<0.005; ^{ns}P>0.05=not significant.

(C) Western blot analysis of caspase-1 and caspase-8 activation at the indicated time points in *Salmonella* SL1344 (MOI=50) infected *GsdmD/Bid/Mlkl/Casp3/7/9*^{KO} iBMDMs that had been left untreated or treated with VX-765. Probing for HSP70 served as a loading control.

(D) Schematic of cell death pathway hierarchy in the absence of all known downstream effectors of apoptosis, pyroptosis and necroptosis.

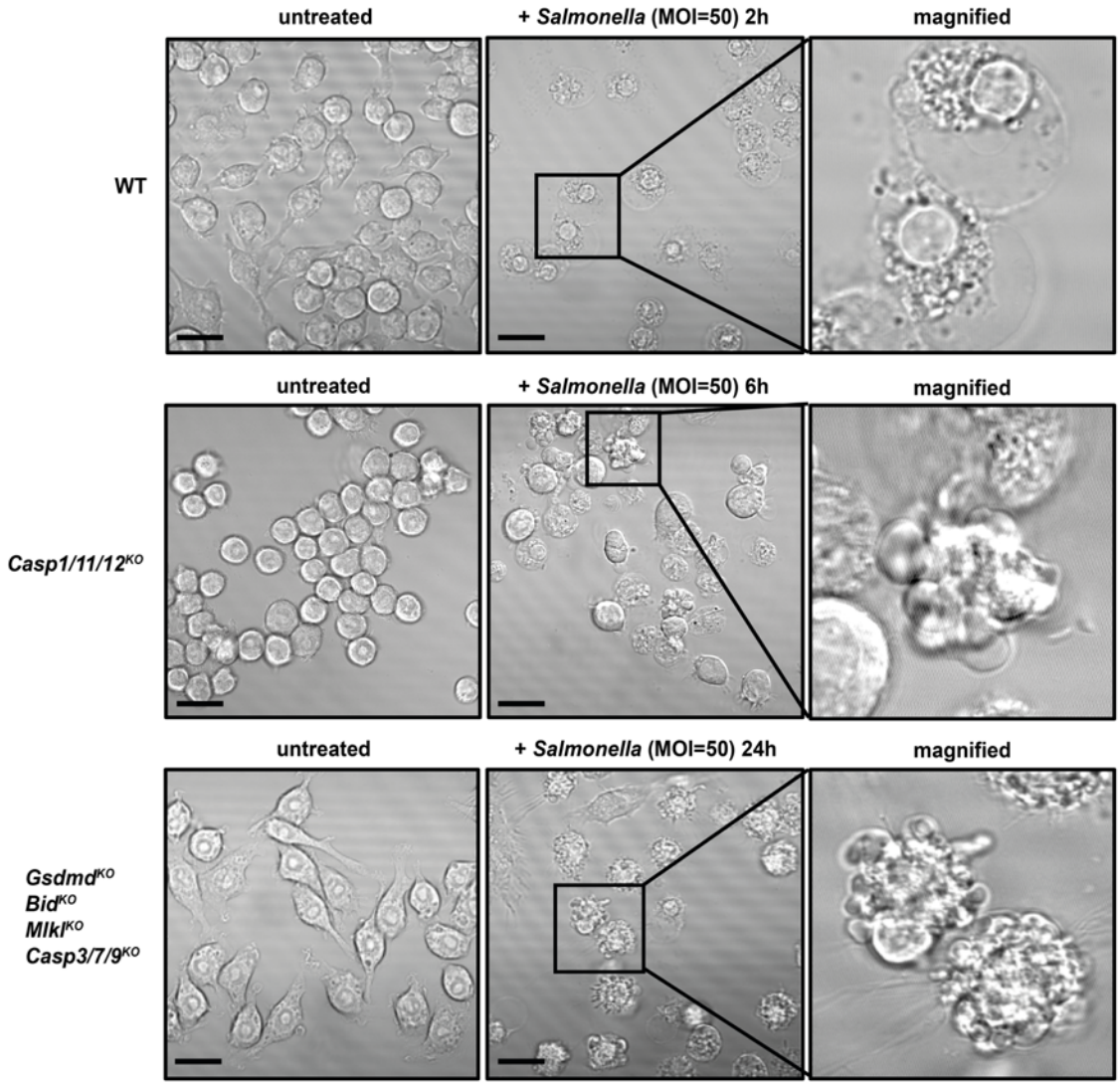

Figure S6. Macrophages Lacking All Downstream Effectors of Caspase-1 and Caspase-8 Undergo Delayed Apoptotic Cell Death upon *Salmonella* Infection.

WT, *Casp1/11/12*^{KO} and *Gsdmd/Bid/Mlkl/Casp3/7/9*^{KO} iBMDM cells were left untreated or infected with *Salmonella* SL1344 (MOI=50) and analyzed using brightfield microscopy. Scale bar: 20 µm.

DISCUSSION

Our findings uncover a highly flexible system of cell death inducing pathways through which phagocytes can purge bacteria from intracellular niches and thereby enable the host to control intracellular bacteria. While we have observed and functionally validated the triggering of the known pathways leading to pyroptosis, necroptosis and apoptosis, our work reveals a remarkable level of plasticity that allows bacterially infected cells to rewire known cell death signaling cascades in surprisingly flexible, thus far unknown ways. We identified caspase-1 and caspase-8 as central pillars of this system and demonstrated that multiple previously unknown versions of rewired cell death circuits can efficiently evict bacteria from intracellular, most likely vacuolar niches as long as one of these central hubs is present.

Our results show that caspase-1, but not caspase-11, can kill *Salmonella* infected cells in the absence of all known effectors of cell killing (i.e. caspases-3,6,7, BID, GSDMD) and that this was mediated via caspase-8. We also observed enhanced cleavage of caspase-8 in *Salmonella* infected iBMDMs that lacked caspase-1, which suggests that the levels of caspase-8 activation may be subject to regulation by the activity of caspase-1. Our data excluded non-redundant roles for ripoptosomes in mediating interactions between these two central regulators of programed cell death and it is likely that ASC provided the molecular link between caspase-1 and caspase-8 as previously shown in different scenarios (Antonopoulos et al., 2015; Lee et al., 2018; Mascarenhas et al., 2017; Pierini et al., 2012; Rauch et al., 2017; Sagulenko et al., 2013; Schneider et al., 2017; Van Opdenbosch et al., 2017). Whether the strong activation of caspase-8 in the absence of caspase-1 is indicative of some bona fide, yet to be uncovered inhibitory effects reminiscent of the role of caspase-8 in preventing necroptosis (Oberst et al., 2011) or rather reflects differential kinetics, whereby the more rapid induction of pyroptosis simply kills cells before caspase-8 is fully activated and thus only becomes appreciable in the absence of

caspase-1, requires further examination. Remarkably this requirement for caspase-8 downstream of caspase-1 was not absolute, as *Salmonella*-infected iBMDMs lacking caspase-8 and RIPK3 still died as long as caspase-9 was present even when the effector caspases-3 and -7 where missing. It is tempting to speculate that caspase-9 was directly activated by caspase-1 through a MOMP independent mechanism under these conditions, as cell death still depended on caspase-1. Regardless of the precise molecular mechanisms underpinning the observed phenomena, our findings highlight a role for caspase-1 as a master regulator in the orchestration of multiple cell death pathways during infection with intracellular pathogens, which bears resemblance to recent data proposing a similar role for caspase-8 during embryonic development (Fritsch et al., 2019; Newton et al., 2019). Importantly, however, host defence can also be maintained in the absence of caspase-1, but this depends on the intactness of the downstream effector machinery that under such conditions is coordinated by caspase-8 instead.

It was also interesting that the various alternative circuits of cell death uncovered here all resulted in morphological features characteristic of apoptosis. Thus, rather than one type of lytic cell death, such as pyroptosis, being compensated for by another form of programmed cellular lysis (i.e. necroptosis), our study and recent work by others (Mascarenhas et al., 2017; Van Opdenbosch et al., 2017) indicate that the absence of lytic cell death appeared to be backed up by apoptosis. This is particularly interesting because lytic and non-lytic types of cell death are believed to differ substantially in their consequences for the host, with the former promoting inflammation while the latter often being referred to as immunologically silent. Yet we found here that *in vivo* control of *Salmonella* proceeded largely undeterred irrespective of these functional differences. More work is required to dissect how the qualitatively different forms of cell death impact on the ultimate clearance of the bacteria through adaptive immune responses mediated by $CD4^+$ T cells and $CD8^+$ T cells (Kupz et al., 2014; Kupz et al., 2012).

A potential 'backup' role for caspase-11 in synergizing, enhancing or even compensating for caspase-1 in host defense against intracellular pathogens has been the focus of previous studies (Broz et al., 2012; Ng and Monack, 2013). Our data indicate that caspase-11 can indeed play a minor role in pathogen clearance, not only synergistically with but also independently of caspase-1 and caspase-8. However, caspase-11 could only induce death in some cells upon *Salmonella* infection and this was strictly dependent on the activation of GSDMD, demonstrating its limiting backup ability, compared to caspase-1 which can also kill through caspases-3, -7, -9 and -8 or act as a cell death executioner itself.

Taken together, our work demonstrates a remarkable level of flexibility and plasticity with which macrophages can commit suicide to purge *Salmonella* from intracellular hideouts. As long as caspase-1 or caspase-8 are active, molecular components previously thought to be unique to particular types of programmed cell death can be flexibly rewired and thus ensure the death of *Salmonella*-infected macrophages even when all currently known executioner molecules are absent. Such a complex system has likely arisen as a consequence of host-pathogen co-evolution and the never-ending struggle between pathogens seeking to evade cell death and the host offsetting these attempts through the rewiring of cell death circuits. While we focussed in the present study on a prototypical intracellular pathogen with global relevance, it is interesting to note that extracellular bacterial pathogens, such as *Staphylococcus aureus*, also express and inject effector molecules capable of manipulating apoptosis into host cells through their type VII secretion systems. This suggests that programed cell death may therefore also play an important role in the host response against extracellular bacteria and its is tempting to speculate that the extracellular lifestyle of some bacteria could be considered as yet another evasion strategy of cell death.

ACKNOWLEDGMENTS

We thank M Patsis and G Siciliano for expert animal care; B Helbert and K Mackwell for genotyping; S Monard and his team for help with flow cytometry; V Dixit and N Kayagaki for insightful discussions and all the members of the Herold, Strasser and Bedoui laboratories. This work was supported by grants and fellowships from the Australian National Health and Medical Research Council (NHMRC) (Project Grants 1186575 and 1145728 to MJH, 1143105 to MJH and AS, 1159658 to MJH and SB, Program Grant 1016701 to AS and Fellowships 1020363 to AS, 1156095 to MJH), the Leukemia and Lymphoma Society of America (LLS SCOR 7001-13 to AS and MJH), the Cancer Council of Victoria (project grant 1147328 to MJH, 1052309 to AS and Venture Grant to MJH and AS), the CASS Foundation (to MD), Wellcome Trust Investigator award 108045/Z/15/Z (to CB) as well as by operational infrastructure grants through the Australian Government Independent Research Institute Infrastructure Support Scheme (361646 and 9000220) and the Victorian State Government Operational Infrastructure Support Program.

AUTHOR CONTRIBUTIONS

MJH, AS and SB conceived the study and MJH, AS, SB and MD wrote the manuscript with input from all other authors, MD designed and performed experiments and generated the figures, YD generated the CRISPR iBMDM lines and contributed to experiments, PW, SE, AB, EG, SW, NW, CY, MP, RAS and GE performed and analyzed experiments, RS performed *in vivo* and *in vitro* experiments, NG and SMB performed and KR supervised microscopy, AJK and LT generated CRISPR reagents, ALG performed the bioinformatics, MAD performed the BAX activation assay, DDN provided reagents, JSP, CB, RAS, JEV and MP contributed to experimental design.

COMPETING INTERESTS

The authors declare no competing interests.

STAR METHODS

KEY RESOURCES TABLE

REAGENT or RESOURCE	SOURCE	IDENTIFIER
Antibodies		
rat anti-caspase-11 (4E11)	WEHI	N/A
rat anti-caspase-1 (1H11)	WEHI	N/A
rat anti-BID (2D1-3)	WEHI	N/A
mouse anti-PARP (C2-10)	Santa Cruz	Cat# sc-53643; RRID: AB_785086
rabbit anti-GSDMD	Abcam	Cat# EPR19828; RRID: AB_2783550
rabbit anti-Bak	Sigma Aldrich	Cat# B-5897; RRID: AB_258581
rat anti-Bax (5B7)	WEHI	N/A
Rabbit polyclonal anti-BAX NT	Merck Millipore	Cat#ABC11; RRID: AB_310143
anti-BAX antibody 6A7 (aa113-19)	BD Biosciences	Cat# 556467; RRID: AB_396430
rabbit anti-caspase-9 (10-1-87)	WEHI	N/A
rabbit anti-caspase-7 (D2Q3L)	CST	Cat# 12827S; RRID: AB_2687912
rabbit anti-cleaved caspase-3 (Asp175)	CST	Cat# 9661S; RRID: B_2341188
rabbit anti-RIPK3	ProSci	Cat# 2283; RRID: AB_203256
rabbit anti-cleaved caspase-8 (D5B2)	CST	Cat# 8592S; RRID: AB_10891784
rat anti-caspase-8 (3B10)	WEHI	N/A
rabbit anti-phospho MLKL (S345)	Abcam	Cat# ab196436; RRID: RRID: AB_2687465
rat anti-MLKL (3H1)	Merck	Cat# MABC604; RRID: RRID: AB_2820284
anti-β-actin-HRP (13E5)	CST	Cat# 5125S; RRID: RRID: AB_1903890
mouse anti-HSP70 (BRM-22)	Sigma Aldrich	Cat# MA1-91159; RRID: RRID: AB_1957733
Goat anti-rabbit Ig (H/L): HRP conjugate	Southern Biotech	Cat# 4010-05; RRID: AB_2632593
Goat anti-rat Ig (H/L): HRP conjugate	Southern Biotech	Cat# 3010-05; RRID: AB_619911
Goat anti-mouse Ig (H/L): HRP conjugate	Southern Biotech	Cat# 1010-05; RRID: AB_609673

Goat anti-rabbit Ig (Fc): HRP conjugate	Southern Biotech	Cat# 3030-05; RRID: AB_2716837
Bacterial and Virus Strains		
Stbl3 chemically competent *E. coli*	Invitrogen	Cat# C737303
Chemicals, Peptides, and Recombinant Proteins		
Gentamycin	Sigma Aldrich	Cat# G-1397
ABT-199 (Venetoclax) (BCL-2i)	ActiveBiochem	Cat# A-1231
S63845 (MCL-1i)	ActiveBiochem	Cat# A-6044
A1331852 (BCL-XLi)	ActiveBiochem	Cat# A-6046
Etoposide	Sigma Aldrich	Cat# E-1383
RIP1 inhibitor II, 7-Cl-O-Nec (10mg) (Nec1s)	Merck	Cat# 5.04297.0001
TNFα	Miltenyi	Cat# 130-101-690
Birinapant	TetraLogic/Medivir	N/A
Emricasan	MedKoo	Cat# 510230
VX-765	InvivoGen	Cat# inh-vx765i-1
PhosSTOP phosphatase inhibitor	Roche	Cat# 04906837001
EDTA-free Protease inhibitor cocktail	Roche	Cat# 11836170001
Proteinase K	Roche	Cat# 3115879
dox hyclate	Sigma-Aldrich	Cat# D-9891
Luminata Forte Western HRP substrate	Merck Millipore	Cat# WBLUF0500
Lipopolysaccharide from *E.coli*	Sigma-Aldrich	Cat# L-2880
Critical Commercial Assays		
Promega CyTox LDH assay	Promega	Cat# G1780
Experimental Models: Cell Lines		
Primary murine BMDMs	this manuscript	N/A
murine WT iBMDMs	De Nardo et al 2018	N/A
murine *Casp1/11/12*^{KO} iBMDMs	this manuscript	N/A
murine *Casp1/11/12/8/RipK3*^{KO} iBMDMs	this manuscript	N/A
murine *Casp8/RipK3*^{KO} iBMDMs	this manuscript	N/A
murine *MLKL*^{KO} iBMDMs	this manuscript	N/A
murine *Casp1/8/RipK3*^{KO} iBMDMs	this manuscript	N/A
murine *Casp1/11/8/RipK3*^{KO} iBMDMs	this manuscript	N/A
murine *Casp1/8/RipK3/Gsdmd*^{KO} iBMDMs	this manuscript	N/A
murine *Gsdmd*^{KO} iBMDMs	this manuscript	N/A
murine *Gsdmd/Casp8/Ripk3*^{KO} iBMDMs	this manuscript	N/A
murine *Gsdmd/Casp8/Ripk3/Bax/Bak*^{KO} iBMDMs	this manuscript	N/A
murine *Gsdmd/Casp8/Ripk3/Mlkl/Casp3/7*^{KO} iBMDMs	this manuscript	N/A

murine *Gsdmd/Casp8/Ripk3/Mlkl/Casp3/6/7*^{KO} iBMDMs	this manuscript	N/A
murine *Gsdmd/Casp8/Ripk3/Mlkl/Casp3/7/9*^{KO} iBMDMs	this manuscript	N/A
murine *Gsdmd/Bid/Mlkl/Casp3/7/9*^{KO} iBMDMs	this manuscript	N/A
murine *Gsdmd/Bid/Mlkl/Casp3/6/7/9*^{KO} iBMDMs	this manuscript	N/A
murine *Gsdmd/Bid/Mlkl/Casp1/3/7/9*^{KO} iBMDMs	this manuscript	N/A
Experimental Models: Organisms/Strains		
Mice: C57BL/6 (WT)	WEHI	N/A
Mice: *MLKL*$^{-/-}$	(Murphy et al., 2013)	N/A
Mice: *Casp1/11*$^{-/-}$	(Kuida et al., 1995)	N/A
Mice: *Casp1/11/12*$^{-/-}$	(Salvamoser et al., 2019)	N/A
Mice: *Casp1/11/12/Ripk3*$^{-/-}$	this manuscript	N/A
Mice: *Casp1/11/12/8/Ripk3*$^{-/-}$	this manuscript	N/A
Mice: *Casp8/Ripk3*$^{-/-}$	(Oberst et al., 2011)	N/A
Salmonella Typhimurium: SL1344	ATCC	Cat#14028
Salmonella Typhimurium: *ΔAroA*	(Kupz et al., 2014)	N/A
Salmonella Typhimurium: SL1344 SPI2 *ssaG-GFP+*	(Hautefort et al., 2003)	N/A
Recombinant DNA		
pVSVg plasmid	Addgene	Cat# 8454
pMDLg/pRRE plasmid	Addgene	Cat# 12251
pRSV-Rev plasmid	Addgene	Cat# 12253
pFH1tUTG- H1-Tet-sgRNA plasmid	(Aubrey et al., 2015)	N/A
pFUGW-Cas9mcherry plasmid	(Aubrey et al., 2015)	N/A
Forward Primers for *Caspase-1* sgRNA: 5'-ACTTGCAAACATTACTGCTA-3'	this manuscript	N/A
Reverse Primers for *Caspase-1* sgRNA: 5'-TAGCAGTAATGTTTGCAAGT-3'	this manuscript	N/A
Forward Primers for *Caspase-3* sgRNA: 5'-ATCTCGCTCTGGTACGGATG-3'	this manuscript	N/A
Reverse Primers for *Caspase-3* sgRNA: 5'-CATCCGTACCAGAGCGAGAT-3'	this manuscript	N/A
Forward Primers for *Caspase-6* sgRNA: 5'-TGGCGTCGTATGCGTAAACG-3'	this manuscript	N/A
Reverse Primers for *Caspase-6* sgRNA: 5'-CGTTTACGCATACGACGCCA-3'	this manuscript	N/A

Forward Primers for *Caspase-7* sgRNA: 5'-GCCCACTTATCTGTACCGCA-3'	this manuscript	N/A
Reverse Primers for *Caspase-7* sgRNA: 5'-TGCGGTACAGATAAGTGGGC-3'	this manuscript	N/A
Forward Primers for *Caspase-8* sgRNA: 5'-TAGCTTCTGGGCATCCTCGA-3'	this manuscript	N/A
Reverse Primers for *Caspase-8* sgRNA: 5'-TCGAGGATGCCCAGAAGCTA-3'	this manuscript	N/A
Forward Primers for *Caspase-9* sgRNA: 5'-AACTTGAGCACCGATTCCGC-3'	this manuscript	N/A
Reverse Primers for *Caspase-9* sgRNA: 5'-GCGGAATCGGTGCTCAAGTT-3'	this manuscript	N/A
Forward Primers for *Caspase-11* sgRNA: 5'- AGCCTTTCGTGTACGGCCAT -3'	this manuscript	N/A
Reverse Primers for *Caspase-11* sgRNA: 5'- ATGGCCGTACACGAAAGGCT -3'	this manuscript	N/A
Forward Primers for *Caspase-12* sgRNA: 5'-TGCGAGTTTCATCCTGAACA-3'	this manuscript	N/A
Reverse Primers for *Caspase-12* sgRNA: 5'-TGTTCAGGATGAAACTCGCA-3'	this manuscript	N/A
Forward Primers for *Ripk3* sgRNA: 5'-GGAACCGCTGACGCACCAGT-3'	this manuscript	N/A
Reverse Primers for *Ripk3* sgRNA: 5'-ACTGGTGCGTCAGCGGTTCC-3'	this manuscript	N/A
Forward Primers for *Gsdmd* sgRNA: 5'-CAGAGGCGATCTCATTCCGG-3'	this manuscript	N/A
Reverse Primers for *Gsdmd* sgRNA: 5'-CCGGAATGAGATCGCCTCTG-3'	this manuscript	N/A
Forward Primers for *Bid* sgRNA: 5'-GGTCAGCAACGGTTCCGGCC-3'	this manuscript	N/A
Reverse Primers for *Bid* sgRNA: 5'-GGCCGGAACCGTTGCTGACC-3'	this manuscript	N/A
Forward Primers for *Mlkl* sgRNA: 5'-TACCCAACACTTTCGGCCTG-3'	this manuscript	N/A
Reverse Primers for *Mlkl* sgRNA: 5'-CAGGCCGAAAGTGTTGGGTA-3'	this manuscript	N/A
Forward Primers for *Caspase12* indel sequencing: 5'-TTACAGCCAGGAGGACACAT-3'	this manuscript	N/A
Reverse Primers for *Caspase12* indel sequencing: 5'-ACAGTCTAAGGGATATGGGG-3'	this manuscript	N/A
Software and Algorithms		
GraphPad Prism	Version 7.0d; GraphPad Software Inc.	https://www.graphpad.com/scientific-software/prism/
Image Lab	Version 6.0.0	Bio-Rad laboratories

Adobe Illustrator CC	Version 2015.1.0	http://www.adobe.com/Illustrator
Fiji	Version 2.0.0-rc-69/1.52v	ImageJ: https://imagej.net/Fiji
IMARIS	Version 9.5	Oxford Instruments - Imaris
edgeR	(Robinson et al., 2010)	N/A
Other		
Protein G Sepharose® 4 fastflow	GE Healthcare	Cat#17-0618-01

CONTACT FOR REAGENT AND RESOURCE SHARING

Lead Contact

Further information and requests for resources and reagents should be directed to and will be fulfilled by the Lead Contacts, Andreas Strasser (strasser@wehi.edu.au) and Marco Herold (herold@wehi.edu.au).

Materials Availability

Unique mouse lines and iBMDM cell lines generated in this study may be obtained (pending continued availability) from the Lead Contact with a completed Materials Transfer Agreement.

Data and Code Availability

The published article includes all datasets generated or analyzed during this study. The full CRISPR/Cas9 whole genome screen dataset supporting the current study may be obtained from the Lead Contact upon request.

EXPERIMENTAL MODEL AND SUBJECT DETAILS

Mice

C57BL/6 (WT), *Mlkl*$^{-/-}$ (Murphy et al., 2013), *Casp8/R3*$^{-/-}$ (Oberst et al., 2011), *Casp1/11*$^{-/-}$ (Kuida et al., 1995), *Casp1/11/12*$^{-/-}$ (Salvamoser et al., 2019), *Casp1/11/12/R3*$^{-/-}$, and

Casp1/11/12/8/R3$^{-/-}$ mice were bred and maintained at The Walter and Eliza Hall Institute of Medical Research Animal Facility. Both age- and sex-matched animals between eight and fourteen weeks of age were used for *in vivo* and *in vitro* studies. All mice were bred and housed in specific pathogen-free facilities, in a 12-hour light/dark cycle in ventilated cages, with free acess to chow and water supply *ad libitum*. All animal experiments were approved by The Walter and Eliza Hall Institute of Medical Research Animal Ethics Committee and The University of Melbourne Animal Ethics Committee (AEC 1714194) and were conducted in accordance with the Prevention of Cruelty to Animals Act (1986) and the Australian National Health and Medical Research Council Code of Practice for the Care and Use of Animals for Scientific Purposes (1997). In accordance with the Prevention of Cruelty to Animals Act (1986) and the Australian National Health and Medical Research Council Code of Practice for the Care and Use of Animals for Scientific Purposes mice were euthanized at a weight loss of more than 15%, which is described in here as 'mouse survival'.

Bone Marrow Chimeras

Bone marrow chimeras were generated as previously described (Bachem et al., 2019). Briefly, C57BL/6-CD45.1 mice were lethally irradiated with 2 doses of 550 rad and reconstituted with 5×10^6 T-cell-depleted bone marrow cells from *Casp1/11/12/8/Ripk3*$^{-/-}$ (C57BL/6-CD45.2) mice. Chimeric mice were allowed to reconstitute for at least 8 weeks before use in experiments.

Bone marrow-derived macrophages (BMDMs)

Bone marrow-derived macrophages (BMDMs) were prepared by flushing bone marrow from femurs and tibiae of both male and female mice, and culturing cells in DMEM supplemented

with 10% fetal bovine serum (FBS; Sigma-Aldrich), 15% L929-conditioned medium, 100 U/mL penicillin and 100 mg/mL streptomycin for six days in non-tissue culture treated dishes.

Immortalized bone marrow-derived macrophages (iBMDMs)

C57BL/6 *Cre-J2* immortalized bone marrow-derived macrophages (iBMDM) (De Nardo et al., 2018) were passaged in DMEM supplemented with 10% FBS, 100 U/mL penicillin and 100 mg/mL streptomycin at 37°C and 10% CO_2. CRISPR/Cas9 mediated gene deletion was achieved as previously described (Aubrey et al., 2015; Kueh and Herold, 2016). In brief, sgRNAs targeting the genes of interest were designed *in silico* and cloned into an inducible lentiviral expression vector. Lentivirus was generated using 293T cells and 1×10^5 target iBMDM cells transduced with the respective virus supernatant. Infected cells were expanded and single cell sorts into tissue culture medium containing 1 µg/mL dox hyclate (to induce sgRNA expression) (Sigma-Aldrich D9891) performed on eGFP and mCherry expressing populations using FACSaria flow cytometer. Single cell clones were expanded and gene deletion confirmed via Western blot analysis of the targeted protein as described above.

Bacterial Strains for *in vivo* and *in vitro* Infection Studies

For *in vivo* infection, *S.* Typhimurium *ΔAroA* was grown shaking at 37ºC in Luria-Bertani (LB) broth supplemented with 50 µg/mL streptomycin for 16 to 18 h, diluted in PBS and 200 CFU were injected into the tail vein in a volume of 200 µL. The number of replicating bacteria was determined by homogenizing organs from infected mice in 5 mL of sterile PBS. The homogenate was serially diluted and plated onto LB agar plates supplemented with 50 µg/mL streptomycin. Plates were incubated at 37º C for 24 h.

S. Typhimurium strain SL1344 was used for *in vitro* infection of primary bone marrow derived macrophages (BMDMs) and immortalized bone marrow macrophages (iBMDMs). SL1344

was grown shaking at 37ºC over night in (LB) broth (+50 µg/mL Streptomycin) for 16 to 18 h and OD_{600} was determined using a spectrophotometer to calculate multiplicity of infection (MOI). For infection, cells were infected with SL1344 at MOI of 50 in serum free and antibiotic free medium. After 1 h, cells were washed twice with warm PBS and medium replaced with serum containing Dulbecco's modified Eagle's medium DMEM with 50 µg/mL Gentamycin to prevent growth of extracellular bacteria.

METHOD DETAILS

Cell Culture

Bone marrow-derived macrophages (BMDMs) were passaged in DMEM supplemented with 10% FBS, 15% L929-conditioned medium, 100 U/mL penicillin and 100 mg/mL streptomycin at 37°C and 10% CO_2. Immortalized bone marrow-derived macrophages (iBMDM) were passaged in DMEM supplemented with 10% FBS, 100 U/mL penicillin and 100 mg/mL streptomycin at 37°C and 10% CO_2. For experimental assays, cells were seeded into 6- or 96-well plates at a density of 3×10^5 or 2×10^4 cells/well, respectively, in antibiotic-free medium and rested for 24 h before infection/treatment and downstream analysis as described below.

Lentiviral Infection and CRISPR/Cas9 Mediated Gene Deletion

CRISPR/Cas9 mediated gene deletion was achieved as previously described (Aubrey et al., 2015; Kueh and Herold, 2016). In brief, sgRNAs targeting the genes of interest were designed *in silico* and cloned into an inducible lentiviral expression vector. Lentivirus was generated using 293T cells and 1×10^5 target iBMDM cells transduced with the respective virus supernatant. Infected cells were expanded and single cell sorts into tissue culture medium containing 1 µg/mL dox hyclate (to induce sgRNA expression) (Sigma-Aldrich D9891) performed on eGFP and mCherry expressing populations using FACSaria flow cytometer.

857 Single cell clones were expanded and gene deletion confirmed via Western blot analysis of the
858 targeted protein as described below or in the case of caspase-12 by Sanger sequencing or NGS
859 as previously described (Aubrey et al 2015) using primers outlined in the Key resources table.
860
861 **LDH Release Cell Death Assay**
862 Viability of uninfected, *Salmonella*-infected and/or inhibitor treated BMDMs and iBMDMs at
863 the indicated time points was determined using the CytoTox 96® Non-Radioactive
864 Cytotoxicity Assay (Promega). The percentage of live cells at each time point was calculated
865 comparing LDH release of surviving cells in *Salmonella*-infected wells to LDH release of non-
866 infected control cells.
867
868 **Western Blotting**
869 To quantify the levels and activation status of a wide range of cell death initiator and effector
870 molecules upon *Salmonella* infection, cells were lysed at the indicated time points by scraping
871 with cell lysis buffer containing 20 mM Tris-HCl, pH 7.5, 135 mM NaCl, 1.5 mM Mg_2Cl,
872 1 mM EGTA, 1% Triton X-100 (Sigma-Aldrich), 10% glycerol, EDTA-free protease inhibitor
873 tablets (Roche, Basel, Switzerland), and phosphatase inhibitor tablets (Roche). Cell lysates
874 were rotated at 4°C for 20 min and then clarified at 4°C at 13,000 g for 15 min. Absolute protein
875 content of clarified lysates was determined by Bradford assay (Bio-Rad, Hercules, CA, USA),
876 and equal quantities (20–50 μg) of total protein were separated under denaturing and reducing
877 conditions (with 5% β-mercaptoethanol) using 4–12% SDS-PAGE gels (Life Technologies).
878 Proteins were transferred onto nitrocellulose membranes, blocked with either 5% skim milk
879 (Devondale, Brunswick, Australia) or 5% BSA (for phospho-proteins) in PBS with 0.05%
880 Tween-20 (PBST) for 1 hr, and detected using the following primary antibodies: rat anti-
881 caspase-11 (WEHI), rat anti-caspase-1 (WEHI), rat anti-MLKL (3H1; available from Merck),

rabbit anti-phospho S345 MLKL (EPR9515[2]; Abcam, Cambridge, UK), rat anti-caspase-8 (3B10; WEHI), rabbit anti-cleaved caspase-8 (D5B2; Cell Signaling Technology), rabbit anti-RIPK3 (ProSci, Poway, CA, USA), rabbit anti-cleaved caspase-3 (Asp175; Cell Signaling Technology), rabbit anti-caspase-7 (D2Q3L, Cell Signalling), rabbit anti-caspase-9 (10-1-87, WEHI), rabbit anti-GSDMD (EPR19828, Abcam), mouse anti-PARP (C2-10, Santa Cruz), rat anti-BID (2D1-3, WEHI), mouse anti-HSP70 (BRM-22, Sigma Alrich) and rabbit anti-β-actin-HRP (Cell Signaling Technology).

HRP-conjugated goat antibodies against mouse, rat or rabbit IgG (Southern Biotech, Birmingham, AL, USA) were applied as a secondary reagent to membranes, which were subsequently incubated with Amersham ECL Prime Western Blotting Detection Reagent (GE Healthcare) and imaged using a ChemiDoc Touch Imaging System (Bio-Rad). Densitometry was performed using Image Lab v.5.2.1 software (Bio-Rad).

Immunoprecipitation of Activated BAX

To determine BAX activation, 3×10^5 WT and *Casp1/11/12/8/R3*$^{-/-}$ primary BMDMs or *Casp1/11/12/8/R3*^{KO} iBMDMs were left untreated, infected with *Salmonella* and/or treated with a combination of BH3-mimetic drugs (2 μM of each BCL-2i ABT-199, MCL-1i S63845, BCL-XLi A1331852) for 16 h and cells then solubilized with 1% CHAPS for 30 min on ice. Lysates were centrifuged at 13,000 g for 5 min and pre-cleared with 25 μL Protein G Sepharose (Amersham Biosciences). Pre-cleared supernatant was then incubated with antibody (4 μg) of 6A7 anti-BAX antibody (aa113-19, BD Biosciences Cat# 556467, RRID: AB_396430) and Protein-G Sepharose for 2 h at 4°C. Unbound proteins were collected and the resin washed with lysis buffer containing up to 0.1% w/v CHAPS. Immunoprecipitated proteins (IP) were eluted by boiling in SDS-containing sample buffer. Immunoprecipitates and pre-IP samples were electrophoresed on SDS-PAGE and immunoblotted for BAX (anti-BAX NT). To avoid signals from immunoglobulin (Ig) light chains in Western blots, Ig heavy chain-specific HRP-

conjugated goat anti-rabbit IgG antibodies (Southern Biotech Cat# 4041-05) were used as secondary reagent, as previously described (Dengler et al., 2019).

Treatment of Cells *in vitro* with BH3 Mimetic Drugs or Etoposide

Primary *Casp1/11/12/8/Ripk3*$^{-/-}$ BMDMs or WT and *Casp1/11/12/8/Ripk3*^{KO} iBMDMs were seeded for LDH assay or BAX activation analysis as indicated above. The following BH3 mimetic drugs were used for the indicated time points at a final concentration of 2 µM: MCL-1i S63845, BCL-2i ABT199, BCL-XLi A1331852. Etoposide (Sigma) was used at a final concentration of 50 µM.

Treatment of Cells *in vitro* with Caspase Inhibitors

Immortalized bone marrow derived macrophages (iBMDM) of the indicated genotypes were passaged and seeded for LDH release cell death assay or Western blot analysis as indicated above. After 24 h, cells were either left untreated, pre-treated with the caspase-1 specific inhibitor VX-765 (20 µM) or the broadspectrum caspase inhibitor Emricasan (20 µM) for 1 h prior to infection with *Salmonella* SL1344 (MOI=50) in the presence of inhibitor. After 1 h, cells were washed twice with warm PBS and fresh medium containing 50 µg/mL Gentamycin and the respective inhibitor added. At the indicated time points, cells were either harvested for Western blot analysis or cell death was measured by LDH release.

Treatment of Cells *in vitro* with LPS

Immortalized bone marrow derived macrophages (iBMDM) of the indicated genotypes were passaged and seeded for Western blot analysis as indicated above. After 24 h, cells were either left untreated or treated with LPS for 4 hours and harvested for Western blot analysis as described above.

Treatment of Cells *in vitro* with the RIPK1 Inhibitor, Nec1s, and/or TNFα plus Birinapant and Emricasan

Immortalized bone marrow derived macrophages (iBMDM) of the indicated genotypes were passaged and seeded for LDH release cell death assay as indicated above. After 24 h, iBMDMs were either left untreated, pre-treated with the RIPK1 specific inhibitor, Nec1s (30 μM), for 1 h prior to infection with *Salmonella* SL1344 (MOI=50) in the continued presence of Nec1s. After 1 h, cells were washed twice with warm PBS and fresh medium containing 50 μg/mL Gentamycin and Nec1s was added. At the indicated time points, cell death was measured by LDH release. In order to verify effective inhibition of RIPK1 by Nec1s, iBMDMs were treated with TNFα (100 ng/mL) + Birinapant (1 μM) + Emricasan (20 μM) with or without Nec1s (30 μM) or Nec1s alone (30 μM) and harvested for LDH cell death assay at the indicated time points.

Brightfield, Confocal and Lattice Light Sheet Microscopy

For confocal and lattice light sheet microscopy, WT, *Casp1/11/12*$^{-/-}$ or *Casp1/11/12/8/R3*$^{-/-}$ BMDMs were seeded into Nunc microscopy chamber slides at a density of 1×10^5 per well using DMEM without phenol red. After 24 h, cells were stained with MitoTracker-Deep Red FM (Thermo) at a final concentration of 50 nM for 30 min, washed twice and infected with GFP-expressing *Salmonella* SPi-2 (kind gift of Strugnell lab, Peter Doherty Institute (Hautefort et al., 2003)) as previously described. After 30 min, cells were again washed twice and fresh medium containing Gentamycin (50 μg/mL) and PI (25 μg/mL; Sigma-Aldrich) was added. Cells were imaged at the Centre for Dynamic Imaging, WEHI, using either a Zeiss LSM 980 or a custom-built Lattice light sheet system constructed as outlined in (Chen et al., 2014). Confocal images were acquired using a 1.2 NA 40x LD-LCI Plan-Apochromat lens (Zeiss) at a temperature of 37°C at 5% CO_2. For lattice light-sheet imaging, illumination at the back

aperture of the excitation objective was focussed through an annular mask of 0.44 inner NA and 0.55 outer NA. Fluorescent emission was collected by detection objective (Nikon, CFI Apo LWD 25XW, 1.1 NA), and detected by sCMOS cameras (Hamamatsu Orca Flash 4.0 v2). Lattice light sheet images were de-skewed and deconvolved using an interative Richardson-Lucy algorithm before visualization. Images were processed using either Fiji or IMARIS software packages.

For Brighfield microscopy, and WT, *Casp1/11/12*^{KO} or *Gsdmd/Bid/Mlkl/casp3/7/9*^{KO} iBMDM cells were seeded into Nunc microscopy chamber slides at a density of 1×10^5 per well using DMEM. Cells were infected with *Salmonella* SL1344 (MOI=50) as described above and images taken on a Zeiss LSM 980. Images were processed using Fiji software package.

CRISPR/Cas9 Whole Genome Guide RNA Library Screen

293T cells were used to generate lentivirus containing the YUSA mouse full genome sgRNA library (Koike-Yusa et al., 2014). *Gsdmd/Bid/Mlkl/casp3/7/9*^{KO} iBMDMs were seeded at a density of 1×10^6 and lentivirally transduced with the sgRNA library. BFP+ cells were sorted using a FACSaria, expanded and seeded into 10 flasks at a density of 2×10^6 cells. The next day, 5 flasks were infected with *Salmonella* SL1344 (MOI=50) as described in the protocols above, and 5 flasks were harvested as non-infection control. Infected flasks were washed every 24 h for 3 days in order to remove cell debris and dying cells, and medium containing Gentamycin replaced respectively. Once surviving cells of each flask had expanded sufficiently, they were split and re-seeded at a density of 1×10^6 cells for a second round of infection. The remaining cells were frozen for analysis of guide RNA enrichment by NGS. This procedure was repeated for a third round. Genomic DNA of harvested cells from control flasks and *Salmonella*-infected flasks was extracted using the Qiagen genomic DNA extraction kit as per the manufacturer's protocol (Qiagen). For targeted PCR of gDNA Insertion Sites,

unique primers were used to amplify from the CRISPR backbone vector which surrounds the guide RNA sequence (Aubrey et al., 2015). Individual infection and control replicates were amplified in triplicate. The PCR cycling conditions were as follows: 95ºC 2 min, (95ºC 15 sec, 60ºC 15 sec, 72ºC 30 sec) x35 cycles, 72ºC 7 min, 4ºC hold step). Amplicon size distribution was ascertained using the Agilent Tapestation D1000 protocol. When a single band was observed at 250 bp, the sample was accepted as amplifying the expected target region. All reactions from the entire plate were then pooled and the PCR amplicons were bead purified as previously described. The quality and integrity of the samples was ascertained as previously described and the concentration was used to set up the sequencing reaction. Each dual indexed library plate pool was quantified using the Agilent Tapestation and the Qubit™ RNA assay kit for Qubit 2.0® Fluorometer (Life Technologies). The indexed pool was diluted to 12 pM for sequencing on a MiSeq instrument as per the manufacturer's instructions. The 150 cycle kit was used to generate a single read of sequence. The fastq sequence output file from the run was used for analysis.

For analysis, the data were formatted into a matrix such that each row represented an individual guide RNA and each column a sample. Analyses of these data were then undertaken using the edgeR (Robinson et al., 2010) software package. Technical replicates were first combined using edgeR's sumTechReps function and water control samples removed prior to data filtering. Guide RNAs were filtered out if they failed to achieve a count of 10 in at least 5 samples, leaving 1384 guides for downstream analysis. Following filtering the data was normalized using edgeR's TMM normalization (Robinson and Oshlack, 2010) with singleton pairing. For normalization only a prior count of 10 was added to all observations. This prior count was then removed for all other analyses. Differential abundance of guide RNAs between the *Salmonella*-infected and control samples was assessed using edgeR's likelihood ratio test. The false discovery rate (FDR) for this analysis was set at 5%. The mean-difference plot was

generated using edgeR's plotMD function, while the heatmap was created using the pheatmap software package.

QUANTIFICATION AND STATISTICAL ANALYSIS

Prism v8.0 (GraphPad Software, San Diego, CA, USA) was used to perform statistical tests. Groups were compared by either unpaired two-tailed t tests for parametric data, or Mann–Whitney tests for non-parametric data. Survival data were analyzed using log rank (Mantel Cox) test. Please refer to the legend of the figures for description of sample size (n) and statistical significance. P values were calculated and are indicated as follows: **P<0.005; *P<0.05; ^{ns}P>0.05=not significant (ns).

REFERENCES

Alvarez-Diaz, S., Dillon, C.P., Lalaoui, N., Tanzer, M.C., Rodriguez, D.A., Lin, A., Lebois, M., Hakem, R., Josefsson, E.C., O'Reilly, L.A*., et al.* (2016). The Pseudokinase MLKL and the Kinase RIPK3 Have Distinct Roles in Autoimmune Disease Caused by Loss of Death-Receptor-Induced Apoptosis. Immunity *45*, 513-526.

Antonopoulos, C., Russo, H.M., El Sanadi, C., Martin, B.N., Li, X., Kaiser, W.J., Mocarski, E.S., and Dubyak, G.R. (2015). Caspase-8 as an Effector and Regulator of NLRP3 Inflammasome Signaling. J. Biol. Chem. *290*, 20167-20184.

Aubrey, B.J., Kelly, G.L., Kueh, A.J., Brennan, M.S., O'Connor, L., Milla, L., Wilcox, S., Tai, L., Strasser, A., and Herold, M.J. (2015). An inducible lentiviral guide RNA platform enables the identification of tumor-essential genes and tumor-promoting mutations in vivo. Cell reports *10*, 1422-1432.

Bachem, A., Makhlouf, C., Binger, K.J., de Souza, D.P., Tull, D., Hochheiser, K., Whitney, P.G., Fernandez-Ruiz, D., Dahling, S., Kastenmuller, W*., et al.* (2019). Microbiota-Derived Short-Chain Fatty Acids Promote the Memory Potential of Antigen-Activated CD8(+) T Cells. Immunity *51*, 285-297 e285.

Bedoui, S., Kupz, A., Wijburg, O.L., Walduck, A.K., Rescigno, M., and Strugnell, R.A. (2010). Different bacterial pathogens, different strategies, yet the aim is the same: evasion of intestinal dendritic cell recognition. Journal of immunology *184*, 2237-2242.

Benoun, J.M., Peres, N.G., Wang, N., Pham, O.H., Rudisill, V.L., Fogassy, Z.N., Whitney, P.G., Fernandez-Ruiz, D., Gebhardt, T., Pham, Q.M*., et al.* (2018). Optimal protection against Salmonella infection requires noncirculating memory. Proceedings of the National Academy of Sciences of the United States of America *115*, 10416-10421.

Browne, A.J., Kashef Hamadani, B.H., Kumaran, E.A.P., Rao, P., Longbottom, J., Harriss, E., Moore, C.E., Dunachie, S., Basnyat, B., Baker, S*., et al.* (2020). Drug-resistant enteric fever worldwide, 1990 to 2018: a systematic review and meta-analysis. BMC Med *18*, 1.

Broz, P., Newton, K., Lamkanfi, M., Mariathasan, S., Dixit, V.M., and Monack, D.M. (2010). Redundant roles for inflammasome receptors NLRP3 and NLRC4 in host defense against Salmonella. J. Exp. Med. *207*, 1745-1755.

Broz, P., Ruby, T., Belhocine, K., Bouley, D.M., Kayagaki, N., Dixit, V.M., and Monack, D.M. (2012). Caspase-11 increases susceptibility to Salmonella infection in the absence of caspase-1. Nature *490*, 288-291.

Chen, B.C., Legant, W.R., Wang, K., Shao, L., Milkie, D.E., Davidson, M.W., Janetopoulos, C., Wu, X.S., Hammer, J.A., 3rd, Liu, Z*., et al.* (2014). Lattice light-sheet microscopy: imaging molecules to embryos at high spatiotemporal resolution. Science *346*, 1257998.

Czabotar, P.E., Lessene, G., Strasser, A., and Adams, J.M. (2014). Control of apoptosis by the BCL-2 protein family: implications for physiology and therapy. Nat. Rev. Mol. Cell Biol. *15*, 49-63.

De Nardo, D., Kalvakolanu, D.V., and Latz, E. (2018). Immortalization of Murine Bone Marrow-Derived Macrophages. Methods Mol Biol *1784*, 35-49.

Dengler, M.A., Robin, A.Y., Gibson, L., Li, M.X., Sandow, J.J., Iyer, S., Webb, A.I., Westphal, D., Dewson, G., and Adams, J.M. (2019). BAX Activation: Mutations Near Its Proposed Non-canonical BH3 Binding Site Reveal Allosteric Changes Controlling Mitochondrial Association. Cell reports *27*, 359-373 e356.

Franchi, L., Amer, A., Body-Malapel, M., Kanneganti, T.D., Ozoren, N., Jagirdar, R., Inohara, N., Vandenabeele, P., Bertin, J., Coyle, A*., et al.* (2006). Cytosolic flagellin requires Ipaf for activation of caspase-1 and interleukin 1beta in salmonella-infected macrophages. Nat. Immunol. *7*, 576-582.

Franchi, L., Eigenbrod, T., Munoz-Planillo, R., and Nunez, G. (2009). The inflammasome: a caspase-1-activation platform that regulates immune responses and disease pathogenesis. Nat. Immunol. *10*, 241-247.

Fritsch, M., Gunther, S.D., Schwarzer, R., Albert, M.C., Schorn, F., Werthenbach, J.P., Schiffmann, L.M., Stair, N., Stocks, H., Seeger, J.M*., et al.* (2019). Caspase-8 is the molecular switch for apoptosis, necroptosis and pyroptosis. Nature *575*, 683-687.
Green, D.R. (2019). The Coming Decade of Cell Death Research: Five Riddles. Cell *177*, 1094-1107.
Hautefort, I., Proenca, M.J., and Hinton, J.C. (2003). Single-copy green fluorescent protein gene fusions allow accurate measurement of Salmonella gene expression in vitro and during infection of mammalian cells. Appl. Environ. Microbiol. *69*, 7480-7491.
Heilig, R., Dilucca, M., Boucher, D., Chen, K.W., Hancz, D., Demarco, B., Shkarina, K., and Broz, P. (2020). Caspase-1 cleaves Bid to release mitochondrial SMAC and drive secondary necrosis in the absence of GSDMD. Life Sci Alliance *3*.
Jorgensen, I., Rayamajhi, M., and Miao, E.A. (2017). Programmed cell death as a defence against infection. Nat. Rev. Immunol. *17*, 151-164.
Kaiser, W.J., Upton, J.W., Long, A.B., Livingston-Rosanoff, D., Daley-Bauer, L.P., Hakem, R., Caspary, T., and Mocarski, E.S. (2011). RIP3 mediates the embryonic lethality of caspase-8-deficient mice. Nature *471*, 368-372.
Kayagaki, N., Stowe, I.B., Lee, B.L., O'Rourke, K., Anderson, K., Warming, S., Cuellar, T., Haley, B., Roose-Girma, M., Phung, Q.T*., et al.* (2015). Caspase-11 cleaves gasdermin D for non-canonical inflammasome signalling. Nature *526*, 666-671.
Koike-Yusa, H., Li, Y., Tan, E.P., Velasco-Herrera Mdel, C., and Yusa, K. (2014). Genome-wide recessive genetic screening in mammalian cells with a lentiviral CRISPR-guide RNA library. Nat. Biotechnol. *32*, 267-273.
Kueh, A.J., and Herold, M.J. (2016). Using CRISPR/Cas9 Technology for Manipulating Cell Death Regulators. Methods Mol Biol *1419*, 253-264.
Kuida, K., Lippke, J.A., Ku, G., Harding, M.W., Livingston, D.J., Su, M.S.-S., and Flavell, R.A. (1995). Altered cytokine export and apoptosis in mice deficient in interleukin-1b converting enzyme. Science *267*, 2000-2003.
Kupz, A., Bedoui, S., and Strugnell, R.A. (2014). Cellular requirements for systemic control of Salmonella enterica serovar Typhimurium infections in mice. Infect. Immun. *82*, 4997-5004.
Kupz, A., Guarda, G., Gebhardt, T., Sander, L.E., Short, K.R., Diavatopoulos, D.A., Wijburg, O.L., Cao, H., Waithman, J.C., Chen, W*., et al.* (2012). NLRC4 inflammasomes in dendritic cells regulate noncognate effector function by memory CD8(+) T cells. Nature immunology *13*, 162-169.
Kupz, A., Scott, T.A., Belz, G.T., Andrews, D.M., Greyer, M., Lew, A.M., Brooks, A.G., Smyth, M.J., Curtiss, R., 3rd, Bedoui, S., and Strugnell, R.A. (2013). Contribution of Thy1+ NK cells to protective IFN-gamma production during Salmonella typhimurium infections. Proceedings of the National Academy of Sciences of the United States of America *110*, 2252-2257.
Lamkanfi, M., and Dixit, V.M. (2014). Mechanisms and functions of inflammasomes. Cell *157*, 1013-1022.
Lee, B.L., Mirrashidi, K.M., Stowe, I.B., Kummerfeld, S.K., Watanabe, C., Haley, B., Cuellar, T.L., Reichelt, M., and Kayagaki, N. (2018). ASC- and caspase-8-dependent apoptotic pathway diverges from the NLRC4 inflammasome in macrophages. Sci Rep *8*, 3788.
Man, S.M., Karki, R., Briard, B., Burton, A., Gingras, S., Pelletier, S., and Kanneganti, T.D. (2017). Differential roles of caspase-1 and caspase-11 in infection and inflammation. Sci Rep *7*, 45126.
Mariathasan, S., Newton, K., Monack, D.M., Vucic, D., French, D.M., Lee, W.P., Roose-Girma, M., Erickson, S., and Dixit, V.M. (2004). Differential activation of the inflammasome by caspase-1 adaptors ASC and Ipaf. Nature *430*, 213-218.
Mascarenhas, D.P.A., Cerqueira, D.M., Pereira, M.S.F., Castanheira, F.V.S., Fernandes, T.D., Manin, G.Z., Cunha, L.D., and Zamboni, D.S. (2017). Inhibition of caspase-1 or gasdermin-D enable caspase-8 activation in the Naip5/NLRC4/ASC inflammasome. PLoS Pathog *13*, e1006502.
Miao, E.A., Leaf, I.A., Treuting, P.M., Mao, D.P., Dors, M., Sarkar, A., Warren, S.E., Wewers, M.D., and Aderem, A. (2010). Caspase-1-induced pyroptosis is an innate immune effector mechanism against intracellular bacteria. Nat. Immunol. *11*, 1136-1142.

Murphy, J.M., Czabotar, P.E., Hildebrand, J.M., Lucet, I.S., Zhang, J.G., Alvarez-Diaz, S., Lewis, R., Lalaoui, N., Metcalf, D., Webb, A.I*., et al.* (2013). The Pseudokinase MLKL Mediates Necroptosis via a Molecular Switch Mechanism. Immunity *39*, 443-453.
Nagata, S. (2018). Apoptosis and Clearance of Apoptotic Cells. Annu. Rev. Immunol. *36*, 489-517.
Newton, K., Wickliffe, K.E., Maltzman, A., Dugger, D.L., Reja, R., Zhang, Y., Roose-Girma, M., Modrusan, Z., Sagolla, M.S., Webster, J.D., and Dixit, V.M. (2019). Activity of caspase-8 determines plasticity between cell death pathways. Nature *575*, 679-682.
Ng, T.M., and Monack, D.M. (2013). Revisiting caspase-11 function in host defense. Cell Host Microbe *14*, 9-14.
Oberst, A., Dillon, C.P., Weinlich, R., McCormick, L.L., Fitzgerald, P., Pop, C., Hakem, R., Salvesen, G.S., and Green, D.R. (2011). Catalytic activity of the caspase-8-FLIP(L) complex inhibits RIPK3-dependent necrosis. Nature *471*, 363-367.
Ofengeim, D., and Yuan, J. (2013). Regulation of RIP1 kinase signalling at the crossroads of inflammation and cell death. Nat. Rev. Mol. Cell Biol. *14*, 727-736.
Orning, P., Weng, D., Starheim, K., Ratner, D., Best, Z., Lee, B., Brooks, A., Xia, S., Wu, H., Kelliher, M.A*., et al.* (2018). Pathogen blockade of TAK1 triggers caspase-8-dependent cleavage of gasdermin D and cell death. Science *362*, 1064-1069.
Pierini, R., Juruj, C., Perret, M., Jones, C.L., Mangeot, P., Weiss, D.S., and Henry, T. (2012). AIM2/ASC triggers caspase-8-dependent apoptosis in Francisella-infected caspase-1-deficient macrophages. Cell Death Differ. *19*, 1709-1721.
Rauch, I., Deets, K.A., Ji, D.X., von Moltke, J., Tenthorey, J.L., Lee, A.Y., Philip, N.H., Ayres, J.S., Brodsky, I.E., Gronert, K., and Vance, R.E. (2017). NAIP-NLRC4 Inflammasomes Coordinate Intestinal Epithelial Cell Expulsion with Eicosanoid and IL-18 Release via Activation of Caspase-1 and -8. Immunity *46*, 649-659.
Robinson, M.D., McCarthy, D.J., and Smyth, G.K. (2010). edgeR: a Bioconductor package for differential expression analysis of digital gene expression data. Bioinformatics *26*, 139-140.
Robinson, M.D., and Oshlack, A. (2010). A scaling normalization method for differential expression analysis of RNA-seq data. Genome Biol *11*, R25.
Sagulenko, V., Thygesen, S.J., Sester, D.P., Idris, A., Cridland, J.A., Vajjhala, P.R., Roberts, T.L., Schroder, K., Vince, J.E., Hill, J.M*., et al.* (2013). AIM2 and NLRP3 inflammasomes activate both apoptotic and pyroptotic death pathways via ASC. Cell Death Differ. *20*, 1149-1160.
Salvamoser, R., Brinkmann, K., O'Reilly, L.A., Whitehead, L., Strasser, A., and Herold, M.J. (2019). Characterisation of mice lacking the inflammatory caspases-1/11/12 reveals no contribution of caspase-12 to cell death and sepsis. Cell Death Differ. *26*, 1124-1137.
Salvesen, G.S., and Dixit, V.M. (1997). Caspases: intracellular signaling by proteolysis. Cell *91*, 443-446.
Schneider, K.S., Gross, C.J., Dreier, R.F., Saller, B.S., Mishra, R., Gorka, O., Heilig, R., Meunier, E., Dick, M.S., Cikovic, T*., et al.* (2017). The Inflammasome Drives GSDMD-Independent Secondary Pyroptosis and IL-1 Release in the Absence of Caspase-1 Protease Activity. Cell reports *21*, 3846-3859.
Shi, J., Zhao, Y., Wang, K., Shi, X., Wang, Y., Huang, H., Zhuang, Y., Cai, T., Wang, F., and Shao, F. (2015). Cleavage of GSDMD by inflammatory caspases determines pyroptotic cell death. Nature *526*, 660-665.
Tenev, T., Bianchi, K., Darding, M., Broemer, M., Langlais, C., Wallberg, F., Zachariou, A., Lopez, J., Macfarlane, M., Cain, K., and Meier, P. (2011). The Ripoptosome, a Signaling Platform that Assembles in Response to Genotoxic Stress and Loss of IAPs. Mol. Cell *43*, 432-448.
Tsuchiya, K., Nakajima, S., Hosojima, S., Thi Nguyen, D., Hattori, T., Manh Le, T., Hori, O., Mahib, M.R., Yamaguchi, Y., Miura, M*., et al.* (2019). Caspase-1 initiates apoptosis in the absence of gasdermin D. Nature communications *10*, 2091.
Van Opdenbosch, N., Van Gorp, H., Verdonckt, M., Saavedra, P.H.V., de Vasconcelos, N.M., Goncalves, A., Vande Walle, L., Demon, D., Matusiak, M., Van Hauwermeiren, F*., et al.* (2017).

Caspase-1 Engagement and TLR-Induced c-FLIP Expression Suppress ASC/Caspase-8-Dependent Apoptosis by Inflammasome Sensors NLRP1b and NLRC4. Cell reports *21*, 3427-3444.
Vandenabeele, P., Galluzzi, L., Vanden Berghe, T., and Kroemer, G. (2010). Molecular mechanisms of necroptosis: an ordered cellular explosion. Nat. Rev. Mol. Cell Biol. *11*, 700-714.
Zhang, L., Chen, S., Ruan, J., Wu, J., Tong, A.B., Yin, Q., Li, Y., David, L., Lu, A., Wang, W.L*., et al.* (2015). Cryo-EM structure of the activated NAIP2-NLRC4 inflammasome reveals nucleated polymerization. Science *350*, 404-409.
Zhao, Y., and Shao, F. (2016). Diverse mechanisms for inflammasome sensing of cytosolic bacteria and bacterial virulence. Curr. Opin. Microbiol. *29*, 37-42.